Mu opioid receptors in GABAergic forebrain neurons moderate motivation for heroin and palatable food

Pauline Charbogne[1,2], Olivier Gardon[1], Elena Martín-García[3], Helen L. Keyworth[4], Aya Matsui[5], Anna E. Mechling[6,7], Thomas Bienert[6], Taufiq Nasseef[2], Anne Robé[1], Luc Moquin[2], Emmanuel Darcq[2], Sami Ben Hamida[2], Patricia Robledo[3], Audrey Matifas[1], Katia Befort[1,10,11], Claire Gavériaux-Ruff[1], Laura-Adela Harsan[6,8,9], Dominik Von Everfeldt[6], Jurgen Hennig[6], Alain Gratton[2], Ian Kitchen[4], Alexis Bailey[4,12], Veronica A. Alvarez[5], Rafael Maldonado[3] and Brigitte L. Kieffer[1,2*].

[1] Institut de Génétique et de Biologie Moléculaire et Cellulaire, CNRS/INSERM/Université de Strasbourg, 1 rue Laurent Fries, 67404 Illkirch, France

[2] Douglas Mental Health Institute, Department of Psychiatry, McGill University, 6875 boulevard LaSalle, H4H 1R3 Montreal, QC, Canada

[3] Departament de Ciencies Experimentals i de la Salut, Universitat Pompeu Fabra, PRBB, C/Dr. Aiguader 88, 08003 Barcelona, Spain

[4] Faculty of Health and Medical Sciences, AY Building, University of Surrey, Guildford, Surrey GU2 7XH, UK

[5] Section on Neuronal Structure, National Institute on Alcohol Abuse and Alcoholism, National Institutes of Health, Bethesda, MD, USA

[6] Department of Radiology, Medical Physics, Medical Center – University of Freiburg, Faculty of Medicine, University of Freiburg, Germany;

[7] Faculty of Biology, University of Freiburg, Freiburg, Germany

[8] Laboratory of Engineering, Informatics and Imaging (ICube), Integrative multimodal imaging in healthcare (IMIS), UMR 7357, University of Strasbourg, France

[9] University Hospital Strasbourg, Department of Biophysics and Nuclear Medicine, Strasbourg, France

Current affiliations:

[10] Laboratoire de Neurosciences Cognitives et Adaptatives (LNCA), Université de Strasbourg Faculté de Psychologie, 12 rue Goethe, F-67000

[11] LNCA UMR 7364, CNRS, 12 rue Goethe, F-67000 Strasbourg

[12] Institute of Medical & Biomedical Education, St. George's University of London, Cranmer Terrace, London, SW17 0RE, UK

* Corresponding author. Douglas Mental Health Institute, Department of Psychiatry, McGill University, 6875 boulevard LaSalle, H4H 1R3 Montreal, QC, Canada
Phone: 514 761-6131 ext.: 3175; fax: 514 762-3033
brigitte.kieffer@douglas.mcgill.ca

Abstract: 243
Article body: 3997
Figures: 4
Tables: 2
Supplemental information: 5

Short title: Mu opioid receptors, striatum and motivation for reward

ABSTRACT

BACKGROUND: Mu opioid receptors (MORs) are central to pain control, drug reward and addictive behaviors, but underlying circuit mechanisms have been poorly explored by genetic approaches. Here we investigate the contribution of MORs expressed in GABAergic forebrain neurons to major biological effects of opiates, and also challenge the canonical disinhibition model of opiate reward.

METHODS: We used Dlx5/6-mediated recombination to create conditional *Oprm1* mice in GABAergic forebrain neurons. We characterized the genetic deletion by histology, electrophysiology and microdialysis, probed neuronal activation by c-Fos immunohistochemistry and resting state-functional magnetic resonance imaging, and investigated main behavioral responses to opiates, including motivation to obtain heroin and palatable food.

RESULTS: Mutant mice showed MOR transcript deletion mainly in the striatum. In the ventral tegmental area (VTA), local MOR activity was intact, and reduced activity was only observed at the level of striatonigral afferents. Heroin-induced neuronal activation was modified at both sites, and whole-brain functional networks were altered in live animals. Morphine analgesia was not altered, neither was physical dependence to chronic morphine. In contrast, locomotor effects of heroin were abolished, and heroin-induced catalepsy was increased. Place preference to heroin was not modified, but remarkably, motivation to obtain heroin and palatable food was enhanced in operant self-administration procedures.

CONCLUSIONS: Our study reveals dissociable MOR functions across mesocorticolimbic networks. Thus beyond a well-established role in reward processing, operating at the level of local VTA neurons, MORs also moderate motivation for appetitive stimuli within forebrain circuits that drive motivated behaviors.

Keywords: mu opioid receptor, conditional gene knockout, opiate, reward, motivation, dopamine.

INTRODUCTION

Mu opioid receptors (MORs) mediate biological effects of morphine and heroin, including their powerful analgesic and euphorigenic properties (1). These receptors are also major players for recreational drug use, contributing to rewarding effects of other drugs of abuse (2) and also mediate naturally pleasurable stimuli including food and social reward (3). Several brain areas responsible for MOR-mediated reward have been identified by intracranial pharmacological manipulations (4), however underlying circuit mechanisms are unclear, and the exact nature of key MOR-expressing neurons remains elusive.

The mesolimbic dopaminergic circuitry is recognized as a main brain network in the processing of appetitive behaviors and drug reward. Central to this circuit is the well characterized ventral tegmental area-nucleus accumbens (VTA-NAc) pathway (5), involving midbrain dopamine (DA) neurons of the VTA projecting massively to GABAergic medium spiny neurons (MSNs) of the ventral striatum, which project back to the VTA either directly or indirectly (6). MORs are densely expressed at both VTA and NAc sites (4, 7), mostly in GABAergic neurons (8-11), and an abundant literature has established that MORs in the VTA are essential for opiate reward (12). In brief, the canonical disinhibition model posits that opiates produce reward by acting at MORs expressed in GABAergic VTA interneurons, an action that in turn relieves the local inhibitory tone and disinhibits dopaminergic neurons (8, 13). However MORs are expressed at multiple pre- and postsynaptic sites within the VTA (14) with distinct synaptic actions on reward, or even aversive (15, 16) processes. In addition, other mechanisms likely contribute and, in particular, MOR agonists are self-administered in VTA, NAc and also elsewhere (4, 12), and heroin is self-administered even in the absence of dopamine terminals in the NAc (17). Here we tested whether MORs expressed in GABAergic forebrain neurons contribute to central effects of opiates with particular emphasis on opiate reward.

METHODS AND MATERIALS

Drugs. See Supplemental Information.

Mutant animals. Dlx-MOR mice were created by breeding our floxed *Oprm1* (*Oprm1*$^{fl/fl}$) mice (18) with Dlx5/6-Cre mice (19), obtained from Beat Lutz (Institute of Physiological Chemistry, Johannes Gutenberg University, Germany) in our vivarium. Details in Supplemental Information.

mRNA analyses. *In situ hybridization in wild type mice.* See Supplemental Information. *Quantitative real-time PCR.* RNA extraction, reverse transcription and cDNA quantification were performed as previously described (20, 21), and detailed in Supplemental Information.

Autoradiographic binding. Ctl, Dlx-MOR and constitutive males and females KO mouse brains were used for determination of total binding for MORs using [^{3}H]DAMGO (D-Ala^2-MePhe^4-Gly-ol^5 enkephalin). MOR binding was carried out as described previously (22) with minor modifications (details in Supplemental Information).

Electrophysiology. Electrophysiology was performed as described previously (23). See Supplemental Information for details.

C-Fos protein immunoreactivity. See Supplemental Information.

Resting-state functional Magnetic Resonance Imaging. Animal preparation, data acquisition and analysis were performed as described previously (24, 25), and directionality analysis conducted as described in Supplemental Information.

Dopamine microdialysis. DA microdialysis after cocaine and heroin administration were performed as described in Supplemental Information. Only mice with correct probe placements (see Supplemental Figure S4) were used in the study.

Behavior. Nociception (1), physical dependence and withdrawal (1, 26), locomotor activity (20), locomotor sensitization (27), bar test (28), conditioned place preference (CPP) (29) and SA procedures (20, 30, 31) are described in Supplemental Information.

Statistical analyses. Data are presented as mean ± standard error (SEM). Statistical significance was achieved by $p<0.05$. See details in Supplemental Information.

RESULTS

Dlx-MOR mice show a major MOR deletion in the striatum

In the adult mouse striatum, the *Oprm1* mRNA, encoding MOR, is mainly co-expressed with *Drd1* (NAc, 64.71±1.68%; dorsal striatum or DS, 54.96±2.11%) and *Drd2* (NAc, 27.02±1.35%; DS, 37.02±2.11%) or both (NAc, 3.13±0.41%; DS, 3.33±0.70%) transcripts (Figure 1A and Supplemental Figure S1) considered canonical markers of GABAergic MSNs. To inactivate the *Oprm1* gene in these neurons, and preserve MOR expression in local VTA neurons, we bred floxed *Oprm1* mice with Dlx5/6-Cre driver mice that express Cre recombinase in GABAergic forebrain neurons (19, 20). *Oprm1* mRNA level was assessed across the brain of mutants (conditional Dlx-MOR and constitutive CMV-MOR) knockout mice using quantitative real-time (qRT) PCR. *Oprm1* expression was significantly decreased at the level of striatum, including the NAc ($t_2=44.65$, $p<0.001$) and the DS ($t_1=267.5$, $p<0.001$), and was intact in the midbrain, hindbrain and the spinal cord ($p>0.05$; Figure 1B) that do not express Cre recombinase. The transcript was undetectable in all the regions for CMV-MOR mice ($p<0.001$).

Transcripts for other components of the opioid system also expressed in the striatum (delta and kappa opioid receptors, preproenkephalin and preprodynorphin) were otherwise unchanged (p>0.05; Figure 1C).

We next examined MOR binding levels throughout the brain using [^{3}H]DAMGO binding autoradiography, rather than MOR protein by immunohistochemistry as the latter is less reliable in brain tissues. Autoradiograms showed strong receptor deletion in the striatum, whereas binding seemed intact in more posterior sections (Figure 1D). Quantification using one-tailed Mann-Whitney analysis showed significant reduction of [^{3}H]DAMGO binding in the NAc core (U=0, p=0.029) and NAc shell (U=0, p=0.029), and no change was detected in mid/hindbrain areas (p>0.05; Figure 1E). MOR proteins expressed in MSNs are normally transported to ventral pallidum (VP) and VTA, along striatopallidal and striatonigral pathways respectively (6). [^{3}H]DAMGO binding was reduced in the VP of mutant mice (U=0, p= 0.029), but no change could be detected in the VTA (U=1, p=0.057; Figure 1E), likely because MSN-MORs at VTA terminals only represent 10-20% total VTA receptors (14).

We then used VTA slice electrophysiology to determine whether MOR activity is modified at VTA terminals of Dlx-MOR mice. As expected, recordings of local VTA GABA interneurons in Ctl mice showed a significant decrease in the amplitude of evoked IPSCs in response to DAMGO. However these synaptic currents were not inhibited in Dlx-MOR mice (unpaired two-tailed t test, t_{16}=6.645, p<0.001, Figure 1F), demonstrating loss of MOR-mediated inhibition over GABA inputs on these neurons in mutant mice. In contrast, recordings of DA neurons showed similar DAMGO-mediated inhibition of eIPSCs in the two groups (t_{16}=0.257, p=0.80, Figure 1G), supporting the notion that inputs to DA neurons are regulated by MORs expressed by other neuron populations, most likely local GABA neurons (12, 14).

In sum, the data together indicate that Dlx-MOR mice show a major MOR deletion in the striatum. Within VTA, presynaptic MORs on MSN afferents are lacking, while MORs expressed by local VTA interneurons or more dorsal projections are intact (Figure 1H).

Neuronal activity is modified in Dlx-MOR mice

To probe the striatum-VTA circuitry, we tested neuronal reactivity to acute heroin administration at the level of DS, NAc and VTA by c-Fos immunohistochemistry. Two-way ANOVA revealed a significant effect of genotype, treatment, as well as interaction in both the dorsolateral striatum (DLS, genotype $F_{1,20}$=8.032, p=0.010; treatment $F_{1,20}$=4.72, p=0.042; interaction $F_{1,20}$=8.71, p=0.008) and VTA (genotype $F_{1,19}$=8.44, p=0.009; treatment $F_{1,19}$=44.65, p<0.001; interaction $F_{1,19}$=5.70, p=0.028). In the NAc shell, two-way ANOVA revealed genotype and treatment effects (genotype $F_{1,20}$=12.92, p=0.002; treatment $F_{1,20}$=17.72, p<0.001; interaction $F_{1,20}$=1.77, p=0.20). In Ctl animals, Student Newman Keuls (SNK) *post hoc* analysis showed a significant increase of c-Fos in response to heroin treatment in NAc (p<0.001), DLS (p<0.01) and VTA (p<0.001). In mutant animals, heroin-induced c-fos activation was undetectable in NAc and DLS, and reduced in the VTA (SNK p<0.01, Figure 2A, B), indicating perturbed responses to opiates within mesolimbic dopaminergic circuitry. NAc core, dorsomedial, ventrolateral and ventromedial striatum did not respond to heroin for both genotypes (not shown).

We further probed the status of whole-brain network activities in live animals, as previously done in (25). Resting-state functional Magnetic Resonance Imaging (Rs-fMRI) and the analysis of whole-brain connectivity (24) showed that the recruitment of DS, NAc and VTA as functional hubs differed in the brain of Dlx-MOR compared to Ctl mice (Figure 2C). This hypothesis-free Rs-fMRI analysis also identified significant modifications of network hubs at other brain sites (Supplemental Figure S2) indicating that the conditional *Oprm1* gene deletion influences neural network activities within and also beyond the VTA-NAc circuit. Note however that forebrain nodes other than striatal hubs were minimally modified, supporting the notion of a major striatal MOR deletion in the forebrain. Directional analysis of functional connectivity (32, 33) across 6 seed regions confirmed significant modifications of information flow within addiction

circuitry and revealed reversed VTA-DS directionality (Figure 2E), consistent with behavioral modifications found in mutant mice (see legend and discussion).

Dlx-MOR mice show intact morphine analgesia and dependence

We then investigated behavioral responses to opiates. Morphine analgesia was unchanged in Dlx-MOR mice using both spinal and supraspinal nociceptive testing (Figure 3A-C), consistent with intact MOR expression at major brain sites for pain control. Mutant mice were also subjected to a chronic morphine regimen. Naloxone-precipitated withdrawal did not differ from Ctl mice, suggesting that forebrain GABA MORs do not contribute significantly to this massive behavioral adaptation to opiates (Figure 3D and Supplemental Figure S3).

Dlx-MOR mice show modified motor responses to heroin

The striatum is critical for motor functions, therefore we investigated locomotor stimulant effects of heroin, a potent diacetylated morphine derivative. During 2h-recording sessions, heroin dose-dependently increased locomotor activity in Ctl mice, as expected (34), but not in Dlx-MOR mice (Figure 3E). Two-way ANOVA revealed treatment effect ($F_{7,160}$=7.37, p<0.001), genotype effect ($F_{1,160}$=23.79, p<0.001) and interaction (genotype X treatment, $F_{7,160}$=7.44, p<0.001). Bonferroni's multiple comparisons test showed no locomotor effect of heroin in Dlx-MOR mice (p>0.05). Treatment effect in Ctl mice was observed at 6, 8 and 10mg/kg heroin (p<0.01, p<0.05 and p<0.001 respectively) compared to saline-treated groups. Genotype effect was observed at 6 and 10 mg/kg (p<0.05 and p<0.001 respectively). Further, sensitization to heroin-induced hyperlocomotion developed in Ctl mice, as classically reported, but Dlx-MOR mice remained unresponsive to heroin in successive sessions (Figure 3F). Three-way repeated measures ANOVA revealed a genotype effect ($F_{1,78}$=39.51; p<0.001), a treatment effect ($F_{1,78}$=52.91; p<0.001) as well as session X genotype X treatment interaction ($F_{3.085,240.62}$=11.01; p<0.001). SNK *post hoc* analysis between the four groups showed no difference between Ctl

group treated with saline and Dlx-MOR groups (p<0.001). Heroin-treated Ctl group showed a significant difference with the three other groups (p<0.001). Finally heroin-induced catalepsy, typically observed in Ctl mice (28), was potentiated in mutant mice (Figure 3G). Two-way ANOVA revealed genotype effect ($F_{1,116}$=14.78; p=0.002), treatment effect ($F_{3,116}$=39.12; p<0.001) as well as genotype X treatment interaction ($F_{3,116}$=12.78; p<0.001). Bonferroni's multiple comparisons test showed a significant treatment effect at 6 and 10 mg/kg (p<0.001) and a difference between Dlx-MOR and Ctl mice at 10 mg/kg heroin (p<0.001).

Because locomotor activity engages DA neurotransmission in the striatum (35, 36), and compensatory mechanisms in the DA system were described upon constitutive deletion of MOR (37), we examined *Drd1* and *Drd2* mRNA levels in DS and NAc, DA-mediated locomotor activation by amphetamine, and cocaine-induced increase of extracellular NAc dopamine levels, however none of these parameters was modified in Dlx-MOR mice (Supplemental Figure S4).

Striatal MORs, therefore, do not seem to modify basal dopaminergic function; however this particular receptor population is essential for the opiate-mediated regulation of motor function.

Dlx-MOR mice show intact place conditioning to opiates

Next, we focused on opiate reward, defined as a subjective hedonic feeling whose experience leads to increase probability of further action to gain the same stimulus (12). We first used CPP, where drug-context association develops upon non-contingent drug delivery. Dlx-MOR and Ctl mice showed comparable preference for the heroin-paired compartment (Figure 4A): three-way ANOVA showed a conditioning effect ($F_{1,166}$=10.61; p<0.001) and a conditioning X treatment interaction ($F_{3,166}$=3.28; p=0.022), a tendency for a treatment effect ($F_{3,166}$=2.62; p=0.052) and no genotype effect ($F_{1,166}$=0.076; p=0.78). These results suggest overall that forebrain GABAergic MORs are not involved in appetitive effects of opiates, nor do they seem to contribute to context learning.

Opiates, as other drugs of abuse, are known to trigger DA release in the NAc which is traditionally associated to drug reward and CPP (38). We investigated heroin-induced (10 mg/kg) DA release in the NAc using microdialysis. Two-way repeated measures ANOVA analysis revealed a time effect ($F_{15,300}$=5.820; p<0.001) and neither a genotype effect ($F_{1,20}$=0.13; p=0.72) nor genotype X time interaction ($F_{15,300}$=0.73; p=0.76). Two-tailed Mann-Whitney analysis of the area under the curve (AUC, inset) confirmed that heroin significantly increased extracellular NAc DA (U=59, p=0.73) in the two groups over the 3-hour session (Figure 4B and Supplemental Figure S5) in line with the CPP data. We also confirmed the absence of hyperlocomotor activity induced by heroin in Dlx-MOR animals concurrently to microdialysis measures (right inset, AUC, two-tailed unpaired t test, t_{21}=3.064, p=0.006).

Altogether, neither CPP testing nor DA microdialysis allowed detecting any Dlx-MOR phenotype in response to heroin, suggesting that MORs in forebrain GABAergic neurons are not involved in opiate reward. This is in agreement with the broadly accepted disinhibition model of opiate reward (12) and our observation that VTA MORs are mostly intact in Dlx-MOR mice. Whether hedonic reactions to heroin, known to involve the NAc shell (39) are altered in Dlx-MOR mice deserves further investigation.

Dlx-MOR mice show enhanced motivation for heroin

The CPP paradigm evaluates conditioned behaviors essentially driven by drug reward. Operant SA, however, also measures other aspects of drug reinforcement related to the acquisition, maintenance, motivation for, and reinstatement of drug seeking behaviors. Thus, operant responses are not only associated with the primary reward circuit, but also recruit other brain networks interfacing the striatum, which contribute to decision-making and behavioral control (40). We thus tested Dlx-MOR mice for heroin SA (Figure 4C-E and Table 1 for statistics). At the starting high dose (0.1 mg/kg/infusion), Dlx-MOR mice stabilized their nose-poking into active holes to a level significantly higher than Ctl animals (fixed ratio 1, FR1

schedule of reinforcement), resulting in overall higher level of heroin intake (Figure 4C). When the heroin dose was reduced in subsequent sessions (0.05 to 0.006 mg/kg/infusion), the two groups maintained hole discrimination, and increased their nose-poking behavior as expected. Dlx-MOR mice consistently showed a higher number of active nose-pokes (three-way ANOVA, significant at 0.1 and 0.025 mg/kg/infusion) (Figure 4C). When further tested in a progressive ratio schedule of reinforcement (PR), Dlx-MOR mice again nose-poked for heroin more actively and achieved a higher breaking point (two-tailed Mann Whitney, U=48, p=0.0172) (Figure 4D), with breaking point/acquisition ratios differing significantly between genotypes (Ctl 0.49 ± 0.21; Dlx-MOR 3.04 ± 1.33; U-Mann-Whitney= 37.50, p<0.05). Finally, mutant mice gradually decreased their heroin SA under extinction conditions; they reinstated this behavior upon cue exposure while Ctl mice did not (two-tailed Mann Whitney, U=25.50, p<0.001) (Figure 4E). Covariance analysis of cue-induced reinstatement with heroin infusion numbers prior to reinstatement sessions further confirmed significant genotype difference ($F_{1,26}$=6.01, p<0.05).

These data showing a higher breaking point and stronger reinstatement to heroin SA in Dlx-MOR mice indicate that forebrain GABAergic MORs significantly regulate motivation to obtain heroin. Together with CPP data, therefore, SA data suggests that this particular MOR population is not involved in rewarding properties of heroin but rather contributes to motivational aspects of heroin consumption.

Dlx-MOR mice show enhanced motivation for palatable food.

Because the increased motivation of Dlx-MOR mice to seek heroin was particularly striking and novel, we finally investigated whether forebrain GABAergic MORs are involved in motivated behaviors for a natural reward (Figure 4F, G and Table 2 for statistics). We examined acquisition and maintenance of operant responding for chocolate, a highly palatable food reward. Overall operant responding was more frequent for palatable food than for heroin in the two groups, due to low satiety induced by each food pellet compared to powerful and durable

effects of a single heroin infusion. On FR1 schedule, Dlx-MOR mice and their controls acquired and maintained stable operant responding for chocolate-flavored food pellets, with higher nose-poking for Dlx-MOR mice significant at session 5 and 10 (Figure 4F). When shifted to a FR5 schedule of reinforcement, the two groups increased and stabilized their active responses to a higher level, which was significantly greater for Dlx-MOR mice for all the sessions (Figure 4F). Mutant mice also showed more responses in a subsequent PR session (two-tailed Mann Whitney, U=58, p=0.0064) (Figure 4G).

Therefore, as for heroin, Dlx-MOR mice showed a higher motivation to obtain palatable pellets. MORs in GABAergic forebrain neurons therefore also moderate motivation to obtain natural rewards, suggesting that this particular MOR population may generally moderate motivation for appetitive stimuli.

DISCUSSION

In this study, we targeted the *Oprm1* gene in forebrain GABAergic neurons, and obtained a deletion of the MOR mRNA mainly at the level of the striatum while the transcript was intact in mid/hindbrain including the VTA. Our behavioral analysis of these conditional mutant mice shows that this particular MOR population does not mediate morphine analgesia or physical morphine withdrawal, but regulates locomotor and motivational effects of heroin. These results extend our previous study showing that ectopic rescue of MOR expression in striatal pDyn neurons of MOR knockout mice is sufficient to restore locomotor morphine effects and morphine SA, but not morphine analgesia and withdrawal (41), and further substantiate the notion of an essential role for striatal MORs in these specific behavioral responses. In addition, our data further show that these receptors do not contribute to heroin positive reinforcement, but modulate motivation to obtain heroin and food reward, revealing a yet unreported role for MORs within addiction circuits.

In the brain, MOR expression was mostly described in GABAergic neurons, including in the VTA (8, 10), bed nucleus of the stria terminalis (9), VP (42), and striatum (11). Dlx5/6-Cre mice, previously used to delete cannabinoid CB1 (19) and delta opioid (20) receptors in forebrain GABAergic neurons, produced a massive *Oprm1* mRNA deletion in the striatum where MOR and Cre expression overlap, while mRNA levels remained intact elsewhere. In the striatum, MOR transcripts were almost totally deleted in both NAc and DS (93 and 98%), but substantial levels of MOR binding sites were still detectable (30 and 48%). Remaining *Oprm1* mRNA may originate from cholinergic interneurons (43, 44), and remaining protein from presynaptic receptors on glutamatergic projecting neurons from the cortex (45). Overall we conclude that our targeting strategy led to a major MOR deletion in striatal projection neurons, and that behavioral modifications in these mice mainly arise from the lack of striatal MOR activity. Further supporting this conclusion is our observation that network hubs are mainly modified at the level of VTA-striatal seed regions with minimal modifications at cortical level, and also the fact that behavioral responses tested in this study primarily recruit striatal-mediated responses. We cannot exclude, however, that limited MOR deletion also occurred elsewhere in the forebrain but was undetected, and may also partially contribute to behavioral responses that have not been investigated here.

Total *Oprm1* knockout leads to complete suppression of morphine analgesia (1, 46). In this study, Dlx-MOR mice showed intact morphine-induced antinociception for both spinal and supraspinal responses, indicating that MORs in forebrain GABAergic neurons are not implicated in acute morphine analgesia. MORs are expressed throughout nociceptive pathways in the brain, spinal cord and sensory neurons (7) and our data are in accordance with previous studies indicating that major sites for these responses to morphine include periaqueductal gray (PAG) and spinal cord (47) where receptors are spared. Recent attention has focused on the implication of brain reward circuits in chronic pain (48) and a recent study used optogenetic manipulations to show that corticostriatal circuits regulate both nociceptive and affective aspects

of neuropathic pain (49). Dlx-MOR mice responses to persistent pain will therefore be of interest in future investigations.

Physical dependence induced by chronic morphine administration is abolished in total MOR knockout mice (1). Here, morphine-dependent Dlx-MOR mice develop the full spectrum of physical withdrawal signs upon naloxone administration. Main neuronal sites for opioid withdrawal include locus coeruleus and PAG for somatic signs (50, 51). In accordance, our data suggest that striatal MORs do not contribute to the expression of somatic withdrawal signs, or that a minor contribution of these receptors is not detected under our conditions. Whether the aversive states of withdrawal are modified in mutant mice has not been tested, as yet. A recent study showed that expression of opiate withdrawal-associated aversion involves projections from the paraventricular nucleus of the thalamus to the NAc rather than striatal cell bodies (52) and further investigation will be necessary to evaluate if striatal MORs modulate the negative affect of opiate withdrawal.

In mice, acute heroin injection increases locomotor activity (53), and this behavior is not observed in total MOR knockout mice (34). Dlx-MOR mice in this study show no locomotor response to heroin, consistent with the lack of heroin-induced c-fos activation in the NAc shell [Figure 2A, B and (54)]. Further, we observed a weak but significant heroin-induced cataleptic state in Ctl mice (bar test), as reported and well described for morphine in the literature (28), and this effect was dramatically enhanced in Dlx-MOR mutants. It is possible that heroin-induced hyperactivity normally hides catalepsy in Ctl mice, and that heroin catalepsy is unmasked in Dlx-MOR animals that do not show locomotor activation, as suggested in (55). Heroin-induced locomotor activation and catalepsy, therefore, may engage two separated neural mechanisms. Further, mechanisms underlying locomotor effects of heroin have been proposed to involve DA transmission (56, 57). In our study, the lack of heroin locomotor stimulant effects in Dlx-MOR mice, which was observed both during activity testing (Figure 3E) and along the microdialysis experiment (Figure 4B), was not accompanied by any alterations of

extracellular DA levels in the NAc, suggesting that heroin effects on DA transmission in the NAc and locomotor activation are independent processes.

Rewarding and motivational properties of opiates, as measured by CPP and SA procedures, are both abolished in total MOR knockout mice (1, 58, 59). In Dlx-MOR mice, heroin place conditioning was intact, indicating that both opiate reinforcement and opiate-context association are preserved. This is further supported by intact heroin-induced increase of NAc extracellular DA observed in mutant mice. MORs expressed in GABAergic forebrain neurons, therefore, do not contribute to opiate reward. This conclusion is in accordance with broad literature pointing at VTA as a major site for opiate reinforcement [(60, 61) for review see (4)]. It is also in agreement with the well-accepted disinhibition model of opiate reward where MORs expressed in local VTA GABA interneurons (62), which are intact in Dlx-MOR mice, play a central role in opiate reward.

Importantly however, data from the heroin SA experiments reveal a strong phenotype for Dlx-MOR mice. First, operant responding for heroin was slightly enhanced; second, breaking point in the PR schedule was remarkably higher; and third, cue-induced reinstatement readily occurred in mutant but not Ctl mice, demonstrating together higher motivation to gain heroin. The MOR in GABAergic forebrain neurons, therefore, is implicated in motivation for heroin rather than heroin reward. This is in accordance with recent evidence that striatonigral fibers originating from striosomes, and receiving inputs from cortical regions related to motivational control, form a specialized integrative unit within the mesocorticolimbic dopamine circuit (63) and that striatal MORs are specifically expressed in striosomal compartments (7). Further, Dlx-MOR mice also showed enhanced motivation to gain palatable food. This observation strengthens the heroin SA data, and opens the possibility that MORs in forebrain GABAergic neurons play a general role in motivational behaviors that perhaps extends to most forms of reward.

Finally, Dlx-MOR mice represent a unique genetic model, which allows dissociation of rewarding and motivational properties of opiates within the highly complex reward brain networks (64). Also remarkably, modifications of information flow between functional networks detected in live Dlx-MOR mice further support the notion of altered VTA dialogue with dorsal but not ventral striatum. These mutant mice therefore provide support to distinguish liking and wanting components of addiction (65), and position MOR as a player in both aspects. Intriguingly, increased performance of mutant mice to obtain heroin suggests that activation of MOR in forebrain GABAergic neurons normally limits motivation for heroin. We propose that, within corticomesolimbic circuitry, VTA-MORs mediate rewarding properties of opiates as previously established, whereas striatal MORs moderate incentive to gain the appetitive stimulus. The latter MOR function may contribute to homeostatic mechanisms, which possibly minimize transition from recreational to compulsive drug use and reduce abuse liability of drug reward. Our study therefore opens the way to circuit mapping of opioid mechanisms underlying motivation and decision-making (40, 66).

Acknowledgements

We thank Nagina Mahmood and Christine Colley for their assistance with the microdialysis histology and the RNAscope experiment, respectively, Grégoire Maroteaux for help in statistical analyses and Maria Osikowicz for her help with figures. We thank the Mouse Clinical Institute and the animal core facility at the Institut de Génétique et de Biologie Moléculaire et Cellulaire for technical support (Illkirch, France), as well as Aude Villemain at the Douglas Research Centre (Montreal, Qc, Canada). This work was supported by the Centre National de la Recherche Scientifique, Institut National de la Santé et de la Recherche Médicale, and Université de Strasbourg. HLK was supported by an MRC/ESRC interdisciplinary studentship and the British Pharmacological Society" also work supported by Genaddict grant European Commission (Contract Number: LSHMCT2004-005166). We would also like to thank the US National Institutes of Health (National Institute of Drug Addiction, grant #05010 and National Institute on Alcohol Abuse and Alcoholism, grant #16658), the Canada Fund for Innovation and the Canada Research Chairs for financial support. Electrophysiological experiments were funded by the Intramural Programs of National Institute on Alcohol Abuse and Alcoholism and National Institute of Neurological Disorders and Stroke (#ZIA-AA000421) to VAA, Japan Society for Promotion of Science to AM. SA studies were supported by the Intramural Programs of National Institute on Alcohol Abuse and Alcoholism (NIAAA) and National Institute of Neurological Disorders and Stroke Grant ZIA-AA000421, the DG Research of the European Commission FP7 (#HEALTH-2013-602891), the Spanish 'RETICS-Instituto de Salud Carlos III' (#RD12/0028/0023), the Spanish 'Ministerio de Economia y Competitividad' (#SAF-2014-59648P), the 'Plan Nacional Sobre Drogas' (#PNSD-2013-5068) and the Catalan Government 'AGAUR' (#2014-SGR-1547) and 'ICREA-Acadèmia' (2015) to RM. Part of the work was supported by DFG Excellence Cluster EXC-1086 "BrainLinks-BrainTools".

PC and BLK designed the experiments; PC performed and analyzed c-Fos immunoreactivity, qRT-PCR and behavioral assays, except for self-administration procedures

that were designed, performed and analyzed by EMG and RM; OG, AMati contributed to Dlx-MOR mice production and characterization; HLK and AB performed and analyzed autoradiography binding assay with I K; AMats performed and analyzed electrophysiology with VAA; AR and PC performed RNAscope assay. AEM, TB and LAH designed the rsfMRI study and acquired and analyzed the rsfMRI data, DE and JH assisted in rsfMRI data analysis and study design. TN and ED performed the directional analysis of the rsfMRI data. PC and LM performed heroin microdialysis and AG helped for analysis. SBH helped for statistical analysis of behavioral data; PR performed and analyzed the cocaine microdialysis experiment. PC and BLK wrote the paper. All of the authors discussed the results and commented on the manuscript.

FINANCIAL DISCLOSURES

The authors declare no competing financial interests.

ARTICLE INFORMATION

From the Institut de Génétique et de Biologie Moléculaire et Cellulaire (PC, OG, AR, AMati, KB, CGR, BLK), Centre National de la Recherche Scientifique, Institut National de la Santé et de la Recherche Médicale, Université de Strasbourg, Illkirch, France; Douglas Mental Health University Institute, Department of Psychiatry, McGill University, Montreal, QC, Canada (PC, LM, ED, SBH, AG, BLK); Departament de Ciencies Experimentals i de la Salut (EMG, PR, RM), Universitat Pompeu Fabra, Barcelona, Spain; Faculty of Health and Medical Sciences (HLK, IK, AB), Department of Biochemistry and Physiology, University of Surrey, Guildford, Surrey, United Kingdom; Section on Neuronal Structure, National Institute on Alcohol Abuse and Alcoholism, National Institutes of Health (AMats, VAA), Bethesda, MD, USA; Department of Radiology (AEM, TB, LAH, DVE, JH), Medical Physics, Medical Center – University of Freiburg, Faculty of Medicine, University of Freiburg, Germany; Faculty of Biology (AEM), University of Freiburg, Freiburg, Germany; Laboratory of Engineering (LAH), Informatics and Imaging (ICube), Integrative multimodal imaging in healthcare, UMR 7357, University of Strasbourg, France; University Hospital Strasbourg (LAH), Department of Biophysics and Nuclear Medicine, Strasbourg, France; Laboratoire de Neurosciences Cognitives et Adaptatives (KB), Université de Strasbourg, Faculté de Psychologie, Strasbourg, France; LNCA UMR 7364 (KB), CNRS, Strasbourg, France; and Institute of Medical & Biomedical Education (AB), St. George's University of London, London, United Kingdom.

Address correspondence to Brigitte L. Kieffer, Ph.D., Douglas Hospital Research Center, Perry Pavilion Room E-3317.1,6875 Boulevard LaSalle, Montreal, Quebec H4H 1R3,Canada; E-mail: brigitte.kieffer@douglas.mcgill.ca.

REFERENCES

1. Matthes HW, Maldonado R, Simonin F, Valverde O, Slowe S, Kitchen I, et al. (1996): Loss of morphine-induced analgesia, reward effect and withdrawal symptoms in mice lacking the mu-opioid-receptor gene. *Nature*. 383:819-823.

2. Charbogne P, Kieffer BL, Befort K (2014): 15 years of genetic approaches in vivo for addiction research: Opioid receptor and peptide gene knockout in mouse models of drug abuse. *Neuropharmacology*. 76 Pt B:204-217.

3. Moles A, Kieffer BL, D'Amato FR (2004): Deficit in attachment behavior in mice lacking the mu-opioid receptor gene. *Science*. 304:1983-1986.

4. Le Merrer J, Becker JA, Befort K, Kieffer BL (2009): Reward processing by the opioid system in the brain. *Physiol Rev*. 89:1379-1412.

5. Russo SJ, Nestler EJ (2013): The brain reward circuitry in mood disorders. *Nat Rev Neurosci*. 14:609-625.

6. Lobo MK, Karsten SL, Gray M, Geschwind DH, Yang XW (2006): FACS-array profiling of striatal projection neuron subtypes in juvenile and adult mouse brains. *Nat Neurosci*. 9:443-452.

7. Erbs E, Faget L, Scherrer G, Matifas A, Filliol D, Vonesch JL, et al. (2015): A mu-delta opioid receptor brain atlas reveals neuronal co-occurrence in subcortical networks. *Brain Struct Funct*. 220:677-702.

8. Johnson SW, North RA (1992): Opioids excite dopamine neurons by hyperpolarization of local interneurons. *J Neurosci*. 12:483-488.

9. Kudo T, Konno K, Uchigashima M, Yanagawa Y, Sora I, Minami M, et al. (2014): GABAergic neurons in the ventral tegmental area receive dual GABA/enkephalin-mediated inhibitory inputs from the bed nucleus of the stria terminalis. *Eur J Neurosci*. 39:1796-1809.

10. Lowe JD, Bailey CP (2015): Functional selectivity and time-dependence of mu-opioid receptor desensitization at nerve terminals in the mouse ventral tegmental area. *Br J Pharmacol.* 172:469-481.

11. Miura M, Saino-Saito S, Masuda M, Kobayashi K, Aosaki T (2007): Compartment-specific modulation of GABAergic synaptic transmission by mu-opioid receptor in the mouse striatum with green fluorescent protein-expressing dopamine islands. *J Neurosci.* 27:9721-9728.

12. Fields HL, Margolis EB (2015): Understanding opioid reward. *Trends Neurosci.* 38:217-225.

13. Wise RA, Rompre PP (1989): Brain dopamine and reward. *Annu Rev Psychol.* 40:191-225.

14. Matsui A, Jarvie BC, Robinson BG, Hentges ST, Williams JT (2014): Separate GABA afferents to dopamine neurons mediate acute action of opioids, development of tolerance, and expression of withdrawal. *Neuron.* 82:1346-1356.

15. Lammel S, Lim BK, Ran C, Huang KW, Betley MJ, Tye KM, et al. (2012): Input-specific control of reward and aversion in the ventral tegmental area. *Nature.* 491:212-217.

16. Tan KR, Yvon C, Turiault M, Mirzabekov JJ, Doehner J, Labouebe G, et al. (2012): GABA neurons of the VTA drive conditioned place aversion. *Neuron.* 73:1173-1183.

17. Pettit H, Ettenberg A, Bloom F, Koob G (1984): Destruction of dopamine in the nucleus accumbens selectively attenuates cocaine but not heroin self-administration in rats. *Psychopharmacology.* 84:167-173.

18. Weibel R, Reiss D, Karchewski L, Gardon O, Matifas A, Filliol D, et al. (2013): Mu opioid receptors on primary afferent nav1.8 neurons contribute to opiate-induced analgesia: insight from conditional knockout mice. *PLoS One.* 8:e74706.

19. Monory K, Massa F, Egertova M, Eder M, Blaudzun H, Westenbroek R, et al. (2006): The endocannabinoid system controls key epileptogenic circuits in the hippocampus. *Neuron.* 51:455-466.

20. Chu Sin Chung P, Keyworth HL, Martin-Garcia E, Charbogne P, Darcq E, Bailey A, et al. (2015): A novel anxiogenic role for the delta opioid receptor expressed in GABAergic forebrain neurons. *Biol Psychiatry*. 77:404-415.

21. Befort K, Filliol D, Darcq E, Ghate A, Matifas A, Lardenois A, et al. (2008): Gene expression is altered in the lateral hypothalamus upon activation of the mu opioid receptor. *Ann N Y Acad Sci*. 1129:175-184.

22. Slowe SJ, Simonin F, Kieffer B, Kitchen I (1999): Quantitative autoradiography of mu-,delta- and kappa1 opioid receptors in kappa-opioid receptor knockout mice. *Brain Res*. 818:335-345.

23. (!!! INVALID CITATION !!! (11)).

24. Mechling AE, Hubner NS, Lee HL, Hennig J, von Elverfeldt D, Harsan LA (2014): Fine-grained mapping of mouse brain functional connectivity with resting-state fMRI. *Neuroimage*. 96:203-215.

25. Mechling AE AT, Lee H-L, Bienert T, Reisert M, Ben Hamida S, Darcq E, Hennig J, v. Elverfeldt D, Kieffer BL* and Harsan L-AA* (*in press*): Deletion of the mu opioid receptor gene in mice reshapes the reward-aversion connectome. *Proceedings of the National Academy of Sciences*.

26. Berrendero F, Castane A, Ledent C, Parmentier M, Maldonado R, Valverde O (2003): Increase of morphine withdrawal in mice lacking A2a receptors and no changes in CB1/A2a double knockout mice. *Eur J Neurosci*. 17:315-324.

27. Contet C, Filliol D, Matifas A, Kieffer BL (2008): Morphine-induced analgesic tolerance, locomotor sensitization and physical dependence do not require modification of mu opioid receptor, cdk5 and adenylate cyclase activity. *Neuropharmacology*. 54:475-486.

28. Tzschentke TM, Schmidt WJ (1996): Morphine-induced catalepsy is augmented by NMDA receptor antagonists, but is partially attenuated by an AMPA receptor antagonist. *Eur J Pharmacol*. 295:137-146.

29. Le Merrer J, Plaza-Zabala A, Del Boca C, Matifas A, Maldonado R, Kieffer BL (2011): Deletion of the delta opioid receptor gene impairs place conditioning but preserves morphine reinforcement. *Biol Psychiatry*. 69:700-703.

30. Martin-Garcia E, Barbano MF, Galeote L, Maldonado R (2009): New operant model of nicotine-seeking behaviour in mice. *Int J Neuropsychopharmacol*. 12:343-356.

31. Burokas A, Gutierrez-Cuesta J, Martin-Garcia E, Maldonado R (2012): Operant model of frustrated expected reward in mice. *Addict Biol*. 17:770-782.

32. Barnett L, Seth AK (2014): The MVGC multivariate Granger causality toolbox: a new approach to Granger-causal inference. *J Neurosci Methods*. 223:50-68.

33. Zhan Y, Paolicelli RC, Sforazzini F, Weinhard L, Bolasco G, Pagani F, et al. (2014): Deficient neuron-microglia signaling results in impaired functional brain connectivity and social behavior. *Nat Neurosci*. 17:400-406.

34. Contarino A, Picetti R, Matthes HW, Koob GF, Kieffer BL, Gold LH (2002): Lack of reward and locomotor stimulation induced by heroin in mu-opioid receptor-deficient mice. *Eur J Pharmacol*. 446:103-109.

35. Serrano A, Aguilar MA, Manzanedo C, Rodriguez-Arias M, Minarro J (2002): Effects of DA D1 and D2 antagonists on the sensitisation to the motor effects of morphine in mice. *Prog Neuropsychopharmacol Biol Psychiatry*. 26:1263-1271.

36. VanderWende C, Spoerlein MT (1979): Morphine-induced catalepsy in mice. Modification by drugs acting on neurotransmitter systems. *Neuropharmacology*. 18:633-637.

37. Park Y, Ho IK, Fan LW, Loh HH, Ko KH (2001): Region specific increase of dopamine receptor D1/D2 mRNA expression in the brain of mu-opioid receptor knockout mice. *Brain Res*. 894:311-315.

38. Di Chiara G, Bassareo V, Fenu S, De Luca MA, Spina L, Cadoni C, et al. (2004): Dopamine and drug addiction: the nucleus accumbens shell connection. *Neuropharmacology*. 47 Suppl 1:227-241.

39. Castro DC, Berridge KC (2014): Opioid hedonic hotspot in nucleus accumbens shell: mu, delta, and kappa maps for enhancement of sweetness "liking" and "wanting". *J Neurosci.* 34:4239-4250.

40. Koob GF, Volkow ND (2010): Neurocircuitry of addiction. *Neuropsychopharmacology.* 35:217-238.

41. Cui Y, Ostlund SB, James AS, Park CS, Ge W, Roberts KW, et al. (2014): Targeted expression of mu-opioid receptors in a subset of striatal direct-pathway neurons restores opiate reward. *Nat Neurosci.* 17:254-261.

42. Kupchik YM, Scofield MD, Rice KC, Cheng K, Roques BP, Kalivas PW (2014): Cocaine dysregulates opioid gating of GABA neurotransmission in the ventral pallidum. *J Neurosci.* 34:1057-1066.

43. Jabourian M, Venance L, Bourgoin S, Ozon S, Perez S, Godeheu G, et al. (2005): Functional mu opioid receptors are expressed in cholinergic interneurons of the rat dorsal striatum: territorial specificity and diurnal variation. *Eur J Neurosci.* 21:3301-3309.

44. Svingos AL, Colago EE, Pickel VM (2001): Vesicular acetylcholine transporter in the rat nucleus accumbens shell: subcellular distribution and association with mu-opioid receptors. *Synapse.* 40:184-192.

45. O'Donnell P, Grace AA (1995): Synaptic interactions among excitatory afferents to nucleus accumbens neurons: hippocampal gating of prefrontal cortical input. *J Neurosci.* 15:3622-3639.

46. Sora I, Takahashi N, Funada M, Ujike H, Revay RS, Donovan DM, et al. (1997): Opiate receptor knockout mice define mu receptor roles in endogenous nociceptive responses and morphine-induced analgesia. *Proc Natl Acad Sci U S A.* 94:1544-1549.

47. Pasternak GW (2014): Opiate pharmacology and relief of pain. *J Clin Oncol.* 32:1655-1661.

48. Navratilova E, Morimura K, Xie JY, Atcherley CW, Ossipov MH, Porreca F (2016): Positive emotions and brain reward circuits in chronic pain. *J Comp Neurol.* 524:1646-1652.

49. Lee M, Manders TR, Eberle SE, Su C, D'Amour J, Yang R, et al. (2015): Activation of corticostriatal circuitry relieves chronic neuropathic pain. *J Neurosci.* 35:5247-5259.

50. Frenois F, Cador M, Caille S, Stinus L, Le Moine C (2002): Neural correlates of the motivational and somatic components of naloxone-precipitated morphine withdrawal. *Eur J Neurosci.* 16:1377-1389.

51. Williams JT, Christie MJ, Manzoni O (2001): Cellular and synaptic adaptations mediating opioid dependence. *Physiol Rev.* 81:299-343.

52. Zhu Y, Wienecke CF, Nachtrab G, Chen X (2016): A thalamic input to the nucleus accumbens mediates opiate dependence. *Nature.* 530:219-222.

53. Bailey A, Metaxas A, Al-Hasani R, Keyworth HL, Forster DM, Kitchen I (2010): Mouse strain differences in locomotor, sensitisation and rewarding effect of heroin; association with alterations in MOP-r activation and dopamine transporter binding. *Eur J Neurosci.* 31:742-753.

54. Leite-Morris KA, Fukudome EY, Shoeb MH, Kaplan GB (2004): GABA(B) receptor activation in the ventral tegmental area inhibits the acquisition and expression of opiate-induced motor sensitization. *J Pharmacol Exp Ther.* 308:667-678.

55. Barghon R, Protais P, Colboc O, Costentin J (1981): Hypokinesia in mice and catalepsy in rats elicited by morphine associated with antidopaminergic agents, including atypical neuroleptics. *Neurosci Lett.* 27:69-73.

56. Kuribara H (1995): Modification of morphine sensitization by opioid and dopamine receptor antagonists: evaluation by studying ambulation in mice. *Eur J Pharmacol.* 275:251-258.

57. Rodriguez-Arias M, Broseta I, Aguilar MA, Minarro J (2000): Lack of specific effects of selective D(1) and D(2) dopamine antagonists vs. risperidone on morphine-induced hyperactivity. *Pharmacol Biochem Behav.* 66:189-197.

58. Becker A, Grecksch G, Brodemann R, Kraus J, Peters B, Schroeder H, et al. (2000): Morphine self-administration in mu-opioid receptor-deficient mice. *Naunyn Schmiedebergs Arch Pharmacol*. 361:584-589.

59. Sora I, Elmer G, Funada M, Pieper J, Li XF, Hall FS, et al. (2001): Mu opiate receptor gene dose effects on different morphine actions: evidence for differential in vivo mu receptor reserve. *Neuropsychopharmacology*. 25:41-54.

60. Bozarth MA, Wise RA (1981): Intracranial self-administration of morphine into the ventral tegmental area in rats. *Life Sci*. 28:551-555.

61. Devine DP, Wise RA (1994): Self-administration of morphine, DAMGO, and DPDPE into the ventral tegmental area of rats. *J Neurosci*. 14:1978-1984.

62. Fields HL, Hjelmstad GO, Margolis EB, Nicola SM (2007): Ventral tegmental area neurons in learned appetitive behavior and positive reinforcement. *Annu Rev Neurosci*. 30:289-316.

63. Crittenden JR, Tillberg PW, Riad MH, Shima Y, Gerfen CR, Curry J, et al. (2016): Striosome-dendron bouquets highlight a unique striatonigral circuit targeting dopamine-containing neurons. *Proc Natl Acad Sci U S A*. 113:11318-11323.

64. Ikemoto S (2010): Brain reward circuitry beyond the mesolimbic dopamine system: a neurobiological theory. *Neurosci Biobehav Rev*. 35:129-150.

65. Berridge KC, Robinson TE, Aldridge JW (2009): Dissecting components of reward: 'liking', 'wanting', and learning. *Curr Opin Pharmacol*. 9:65-73.

66. Olmstead MC, Ouagazzal AM, Kieffer BL (2009): Mu and delta opioid receptors oppositely regulate motor impulsivity in the signaled nose poke task. *PLoS One*. 4:e4410.

Table 1. Statistical analysis of heroin self-administration data.

	Three-way ANOVA			
	Acquisition 0.1 mg/kg/inf		Acquisition 0.05 mg/kg/inf	
	F-value	*P*-value	*F*-value	*P*-value
Genotype	$F_{(1,26)}$ = 3.61	*0.0685*	$F_{(1,27)}$ = 2.55	*0.122*
Hole	$F_{(1,26)}$ = 20.40	*<0.001*	$F_{(1,27)}$ = 6.27	*0.0187*
Day	$F_{(3,78)}$ = 8.73	*<0.001*	$F_{(2,54)}$ =0.04	*0.961*
Genotype × Hole	$F_{(1,26)}$ = 2.63	*0.117*	$F_{(1,27)}$ = 2.05	*0.164*
Genotype × Day	$F_{(3,78)}$ = 0.36	*0.779*	$F_{(2,54)}$ = 0.43	*0.654*
Hole × Day	$F_{(3,78)}$ = 1.58	*0.202*	$F_{(2,54)}$ = 007	*0.937*
Genotype × Hole × Day	$F_{(3,78)}$ = 7.14	*0.625*	$F_{(2,54)}$ = 058	*0.564*
	Acquisition 0.025 mg/kg/inf		Acquisition 0.0125 mg/kg/inf	
	F-value	*P*-value	*F*-value	*P*-value
Genotype	$F_{(1,2)}$ = 5.44	*0.0274*	$F_{(1,27)}$ = 2.81	*0.105*
Hole	$F_{(1,2)}$ = 10.08	*0.00373*	$F_{(1,27)}$ = 8.64	*0.00667*
Day	$F_{(2,54)}$ = 0.19	*0.824*	$F_{(5,135)}$ = 1.53	*0.184*
Genotype × Hole	$F_{(1,2)}$ = 4.75	*0.0381*	$F_{(1,27)}$ = 1.91	*0.179*
Genotype × Day	$F_{(2,54)}$ = 0.02	*0.976*	$F_{(5,135)}$ = 0.72	*0.610*
Hole × Day	$F_{(2,54)}$ = 0.28	*0.760*	$F_{(5,135)}$ = 1.10	*0.365*
Genotype × Hole × Day	$F_{(2,54)}$ = 0.01	*0.993*	$F_{(5,135)}$ = 1.34	*0.252*

	Acquisition 0.006 mg/kg/inf	
	F-value	*P*-value
Genotype	$F_{(1,27)}$ = 1.92	*0.127*
Hole	$F_{(1,27)}$ = 73.78	*0.00341*
Day	$F_{(3,81)}$ = 25.50	*0.00513*
Genotype × Hole	$F_{(1,27)}$ = 1.94	*0.201*
Genotype × Day	$F_{(3,81)}$ = 1.80	*0.791*
Hole × Day	$F_{(3,81)}$ = 24.30	*0.0213*
Genotype × Hole × Day	$F_{(3,81)}$ = 1.91	*0.737*

Three-way ANOVA with genotype as between-subjects factor and repeated measures in the factors day/experimental phase and hole (active/inactive). See Methods and Materials for details.

Table 2. Statistical analysis of chocolate-flavored pellet self-administration data.

	Three-way ANOVA			
	Acquisition FR1		Acquisition FR5	
	F-value	*P*-value	*F*-value	*P*-value
Genotype	$F_{(1,31)}$ = 2.87	*0.101*	$F_{(1,31)}$ = 6.88	*0.0134*
Hole	$F_{(1,31)}$ = 122.15	<0.001	$F_{(1,31)}$ = 259.91	<0.001
Day	$F_{(9,279)}$ = 31.40	<0.001	$F_{(4,124)}$ = 0.81	*0.524*
Genotype × Hole	$F_{(1,31)}$ = 2.79	*0.105*	$F_{(1,31)}$ = 6.80	*0.0139*
Genotype × Day	$F_{(9,279)}$ = 1.75	*0.0772*	$F_{(4,124)}$ = 1.55	*0.193*
Hole × Day	$F_{(9,279)}$ = 34.46	<0.001	$F_{(4,124)}$ = 0.78	*0.542*
Genotype × Hole × Day	$F_{(9,279)}$ = 1.83	*0.0629*	$F_{(4,124)}$ = 1.56	*0.188*

Three-way ANOVA with genotype as between-subjects factor and repeated measures in the factors day and hole (active/inactive). See Methods and Materials for details.

Figure 1. Dlx-MOR mice lack MORs mainly in striatal MSNs. **(A)** Quantification of triple *in situ* hybridization in mouse striatal sections (details in Supplemental Figure S1) shows major *Oprm1* mRNA co-localization with *Drd1*, *Drd2* or both in NAc and DS. **(B)** Quantitative RT-PCR analysis of *Oprm1* mRNA in microdissected brain regions from Ctl, conditional knockout Dlx-MOR and total knockout CMV-MOR mice reveals complete *Oprm1* deletion specifically in DS and NAc of Dlx-MOR mice. Transcript levels in mutants are expressed relative to Ctl (dotted line, n=3 to 4, in triplicates) and shown in rostrocaudal order. **(C)** Quantitative RT-PCR analysis of *Oprd1*, *Oprk1*, *Penk* and *pDyn* mRNAs in NAc (above) and DS (bellow) shows no change in Dlx-MOR mice (n=3 to 4, in triplicates). **(D)** Representative [^{3}H]DAMGO (MOR agonist) binding autoradiograms of brain sections from Ctl and Dlx-MOR mice reveals complete receptor deletion at the level of striatum (bregma 1.1) but not in a more posterior section (Hb, bregma -1.46). Color bar, relative densities in fmol/mg tissue with non-specific binding at background level. **(E)** Quantification of [^{3}H]DAMGO binding in areas with sufficiently high signal (≥60 fmoles/mg tissue) from the forebrain to spinal cord (n=3 to 4) confirms significant MOR decrease in the NAc and VP. MOR density is also lower in DS and VTA, although this is not significant. **(F, G)** Slice VTA electrophysiology (n=6 to 12). **(F)** In GABA interneurons (yellow), DAMGO (1µM) decreased evoked GABAA IPSCs (eIPSCs) in slices from Ctl but not Dlx-MOR mice, while N_6-CPA (A1 receptor agonist, 1µM) reduced eIPSCs in the two groups. **(G)** In dopamine neurons (blue), DAMGO (1µM) decreased GABAA eIPSCs similarly for Ctl and Dlx-MOR, while N_6-CPA had no significant effect. **(H)** Schematic representation of the MOR deletion within NAc/VTA circuitry of Dlx-MOR mice, as indicated by RNA, protein and electrophysiological analysis. Data are represented as mean + SEM. Blue star, significant genotype effect; one star, $p<0.05$; three stars, $p<0.001$. Serpentine, MOR. Amy, Amygdala; DS, dorsal striatum; DRN, dorsal raphe nucleus; EP, endopiriform nucleus; Hb, habenula (MHb, medial); LH, lateral hypothalamus; NAc, nucleus accumbens (NAcc, core; NAcsh, shell); PAG, periaqueductal gray; PFC, prefrontal cortex; RMTg, rostromedial tegmental area; SC, spinal

cord (LI/II, lamina I/II); SN, substantia nigra; Th, thalamus (ThCL, central lateral; ThCM, central medial; ThIMD, intermediodorsal); VP, ventral pallidum; VTA, ventral tegmental area.

Figure 2. Neuronal activity is modified in Dlx-MOR mice. **(A, B)** Heroin-induced neuronal activation. c-Fos immunohistochemistry (IHC) was performed on brain sections from animals perfused 2h after saline or heroin (10 mg/kg, ip) administration. **(A)** Representative images illustrate c-Fos IHC in the NAcsh, DLS and VTA of Ctl and mutant mice. **(B)** Quantification of c-Fos IHC, expressed as c-Fos-positive cells/mm^2 (bilateral, 4-7 sections/animal, n=5 to 6), shows a treatment effect for Ctl mice in all three regions. For Dlx-MOR mice, heroin-induced increase of c-Fos IHC was detected in VTA but not in NAcsh and DLS, indicating strongest modification in the striatum. **(C, D, E)** Whole-brain functional connectivity in live mice using resting-state functional MRI. High resolution spatial independent component analysis followed by partial correlation in time domain and graph theory identifies functional connectivity (FC) hubs displaying above-mean normalized connectivity strength and diversity, which differ across genotypes. **(C)** Focus on NAc-VTA FC shows two hubs covering NAc (left) detectable in Ctl mice (normalized strength>0.041 and/or diversity>0.966) but not Dlx-MOR mice (normalized strength<0.047 and/or diversity<0.940) and, conversely, two hubs with anatomical correspondence to VTA (right) detected in Dlx-MOR mice (normalized strength>0.047 and/or diversity>0.940) but not Ctl mice (normalized strength<0.041 and/or diversity<0.966). Thus, NAc nodes lose, while VTA nodes gain their hub status, indicating modified relay function between these two brain nodes. (n=10 to 12). **(D, E)** Seed-based Granger causality analysis considering 6 MOR-enriched regions within reward circuitry shows distinct information flow in Ctl and Dlx-MOR mice (see full analysis in Supplemental Figure S2). **(D)** Identification of functional dominant or bi-directionality across NAc, DS and VTA is represented in matrices for Ctl and Dlx-mice. Brain regions on the horizontal axis are sources, and regions on the vertical axis are destination of the information flow and the number of subjects showing a significant

directionality (by 100 permutations) is indicated. Mean conditional Granger causality (C-GC) values represent intensity of information flow for each connection (gradient grey scale). The dominant directionality is determined by comparing both number of significant subjects and mean C-GC for each connection (see Methods). **(E)** Scheme summarizing dominant or bi-directionality in Ctl and Dlx-MOR mice for the 3 seed regions of interest in this study (orange arrows) shows that VTA-DS connectivity is reversed in mutants, consistent with abolished heroin-induced locomotor activation and altered heroin SA, whereas VTA-NAc directional connectivity is unchanged concordant with maintained heroin CPP and heroin-induced DA release in the NAc (see Figure 4). Data are represented as mean + SEM. Black star, significant treatment effect; blue star, significant genotype effect. Two stars, $p<0.01$; three stars, $p<0.001$. DS, dorsal striatum; DLS, dorsolateral striatum; Hb, habenula; NAcsh, nucleus accumbens shell; PFC, prefrontal cortex; PAG, periaqueductal gray; VTA, ventral tegmental area. Scale bar = 100 µm.

Figure 3. Dlx-MOR mice show modified motor responses to heroin. Morphine analgesia was investigated in tail immersion [52°C **(A)**] test, tail flick **(B)** and hot plate **(C)** tests. **(A, B)** Acute thermal nociception in spinal reflex responses is unchanged in mutant mice (cumulative dose-response, ip injections, n=12) **(C)** Also, the three parameters measured in the hot plate test upon ip morphine administration (2 or 5 mg/kg, n=5 to 9) reveal treatment but no genotype effects. **(D)** Physical dependence was induced by repeated injections of ascending doses of morphine (10–100 mg/kg, ip, twice daily, 6 days). Scoring of naloxone-precipitated (1 mg/kg, sc) withdrawal signs shows no genotype difference in the expression of morphine physical dependence (n=9 to 15) (global score) (details in Supplemental Figure S3). **(E)** Dose-dependent heroin-induced locomotor activation in Ctl but not Dlx-MOR mice is shown (mg/kg ip, 2h-session, n=4 to 32). **(F)** Sensitization to the heroin locomotor effect (10 mg/kg ip) develops in Ctl mice only (5X 2h-sessions, n=12 to 32). **(G)** Heroin-induced catalepsy, expressed as latency to

paw withdrawal in the bar test, develops in both Ctl and Dlx-MOR mice, and is enhanced in Dlx-MOR mice at 10 mg/kg (n=8 to 27). Data are represented as mean + or - SEM. Symbols: (A, B) black stars, significant difference to baseline; (C, D, E, G) black stars, significant difference to saline treatment; (E, G) blue star, significant genotype effect; (F) black stars, significant difference to all other groups; # significant time effect session 1 vs session 5 for Ctl 10. One symbol, $p<0.05$; two symbols, $p<0.01$; three symbols, $p<0.001$.

Figure 4. Dlx-MOR mice show enhanced motivation for heroin and palatable food. **(A)** CPP to heroin (mg/kg sc, n=4 to 21), established over 6 conditioning sessions, does not differ between Ctl and Dlx-MOR mice (significant session X treatment interaction). Preference is expressed as % time spent in the drug-paired compartment during pre- (left) and post- (right) conditioning sessions. **(B)** DA microdialysis and concurrent locomotor activation. Heroin (10 mg/kg ip, injected after 120 min, recording during 320 min) increases extracellular DA above baseline in the NAc (Supplemental Figure S4) of Dlx-MOR and Ctl mice, with no genotype effect (n=9 to 13) (left). AUC ([DA] ng/mL, inset) analysis confirms no difference between Dlx-MOR and Ctl. Simultaneous to DA increase, heroin stimulates locomotion in Ctl but not Dlx-MOR mice (right). **(C-E)** Operant responding to heroin (n=11 to 18). **(C)** Both Dlx-MOR and Ctl mice acquire and increase heroin SA with decreasing doses (20 successive 1h-daily sessions, FR1 schedule of reinforcement). SA levels (mean number of infusions/session) are higher in the Dlx-MOR group. Heroin SA is significantly higher at 2 doses (dose-response analysis, inset). **(D)** Dlx-MOR mice achieve a higher breaking point in a 3h-PR session (0.0125 mg/kg/inf). **(E)** After extinction (1h-daily sessions for 13 days), Dlx-MOR but not Ctl mice reinstate heroin SA (0.006 mg/kg/inf) upon cue presentation (CIR). **(F, G)** Operant responding to chocolate-flavored pellets (n=20 Ctl, 13 Dlx-MOR). **(F)** Acquisition and maintenance of active nose-poking for chocolate reinforcement is shown (mean number of nose-pokes during 10 days FR1 and 5 days FR5 schedule of reinforcement, 1h-daily sessions). In both FR1 and FR5 sessions, Dlx-MOR mice

show higher operant responding than Ctl mice. **(G)** Breaking-point for chocolate-flavored pellets is higher in mutant mice (5h PR session). Data are represented as mean + or - SEM. Black star, significant treatment effect; blue star, significant genotype effect. #, significant time effect. One symbol, $p<0.05$; two symbols, $p<0.01$; three symbols, $p<0.001$. AUC, area under the curve; CIR, cue-induced reinstatement; FR, fixed ratio; PR, progressive ratio. See Tables 1 and 2 for statistical analysis of SA experiments.

Figure 1

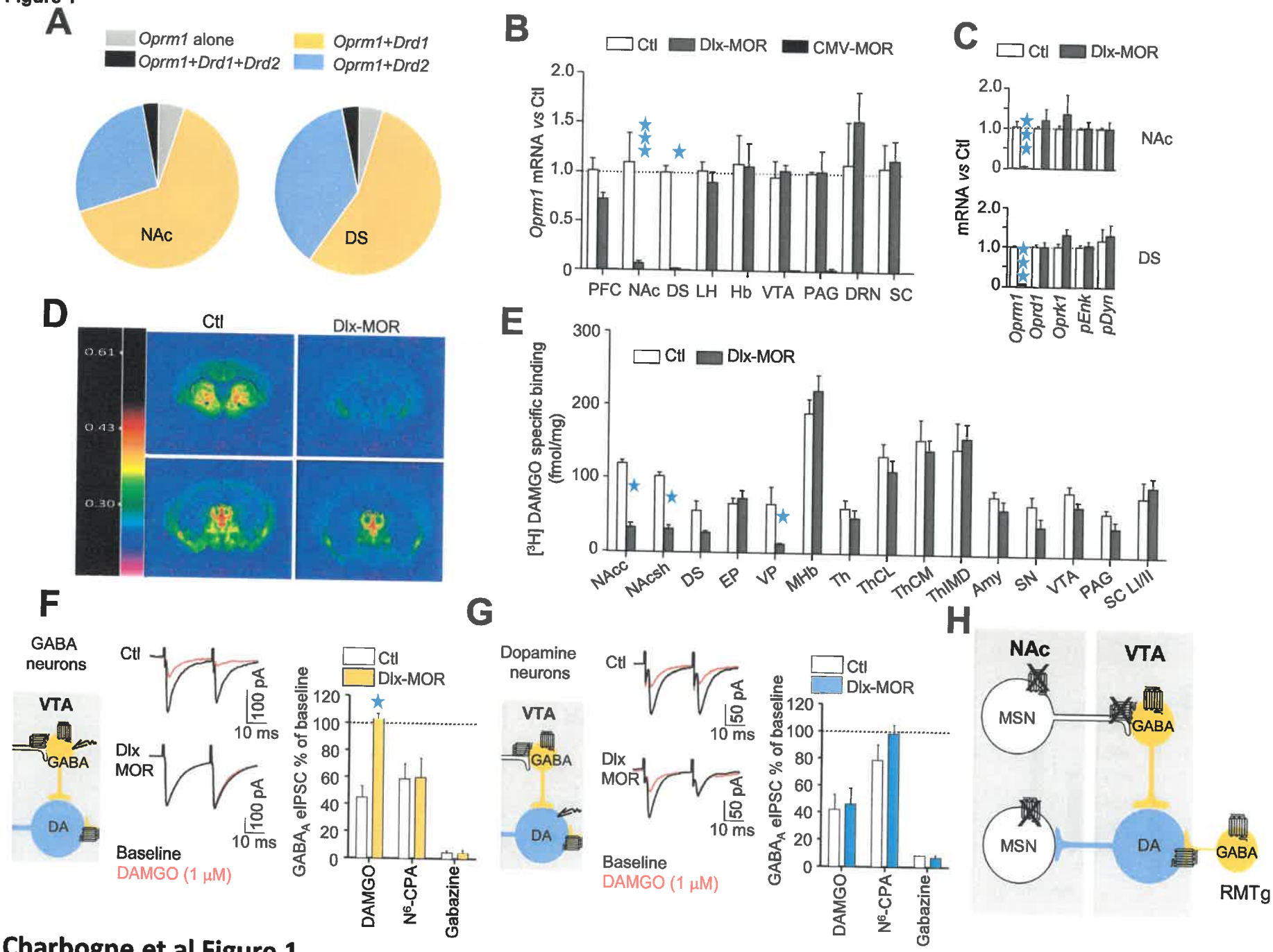

Charbogne et al Figure 1

Figure 2

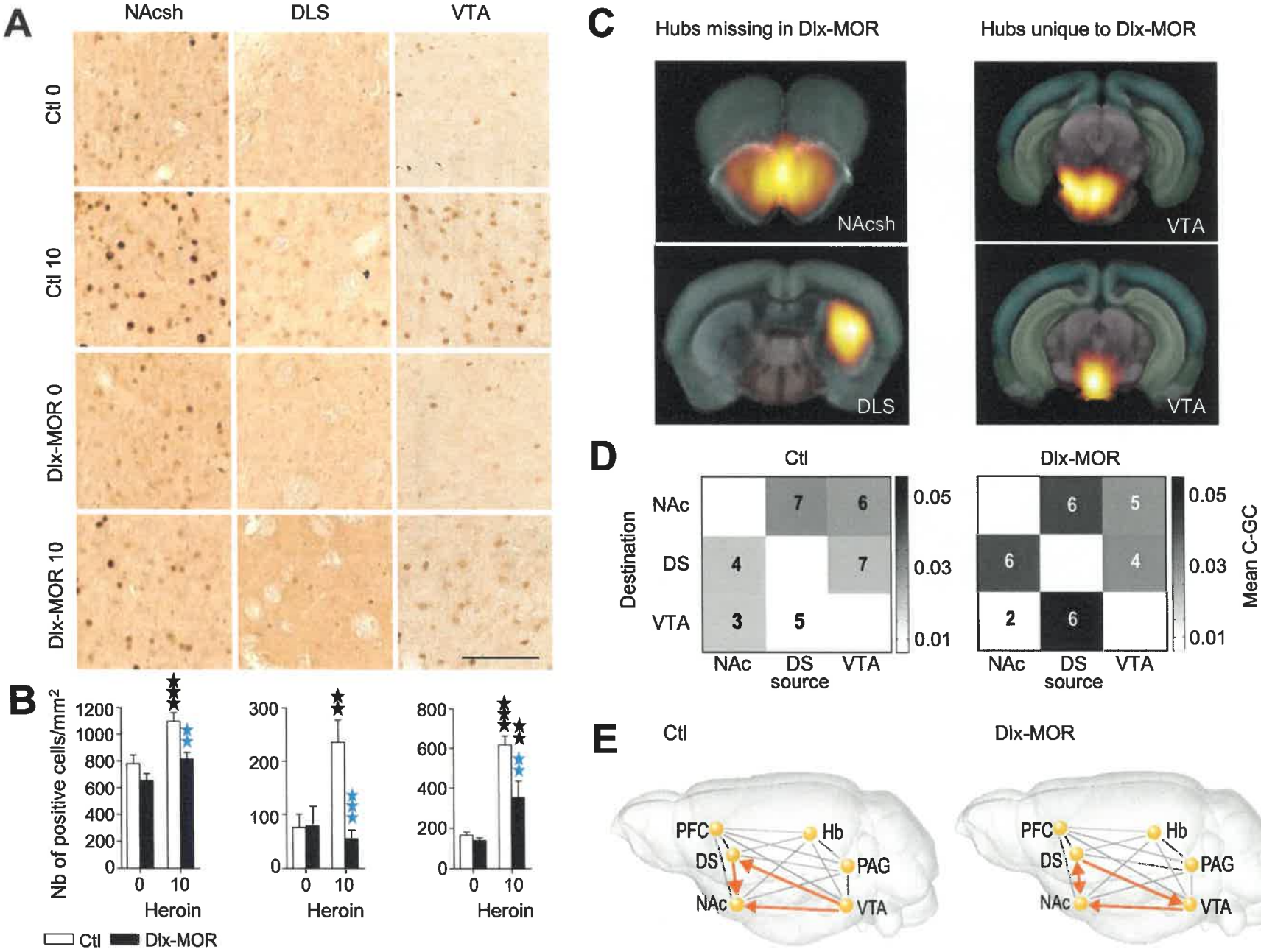

Charbogne et al Figure 2

Figure 3

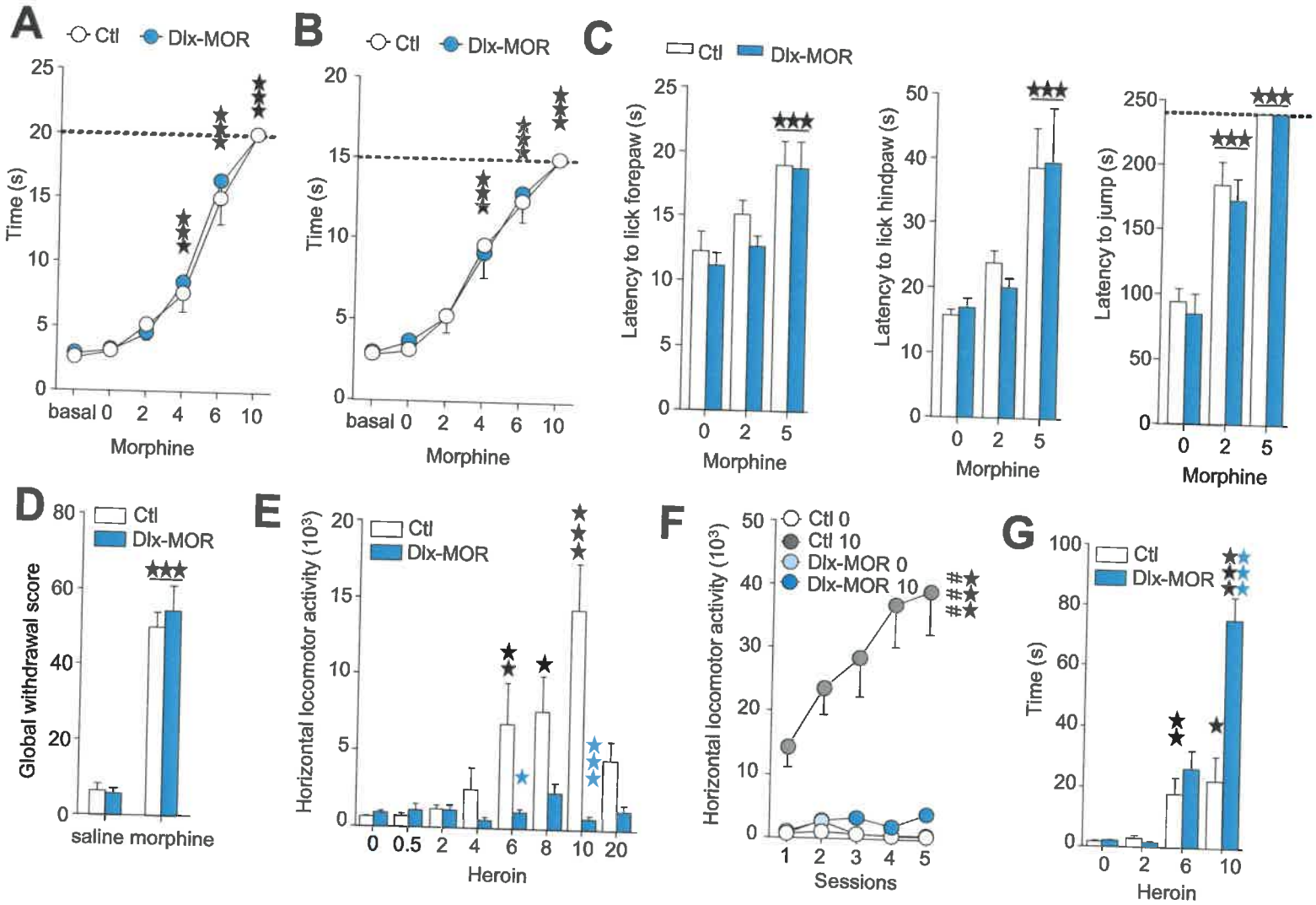

Charbogne et al Figure 3

Figure 4

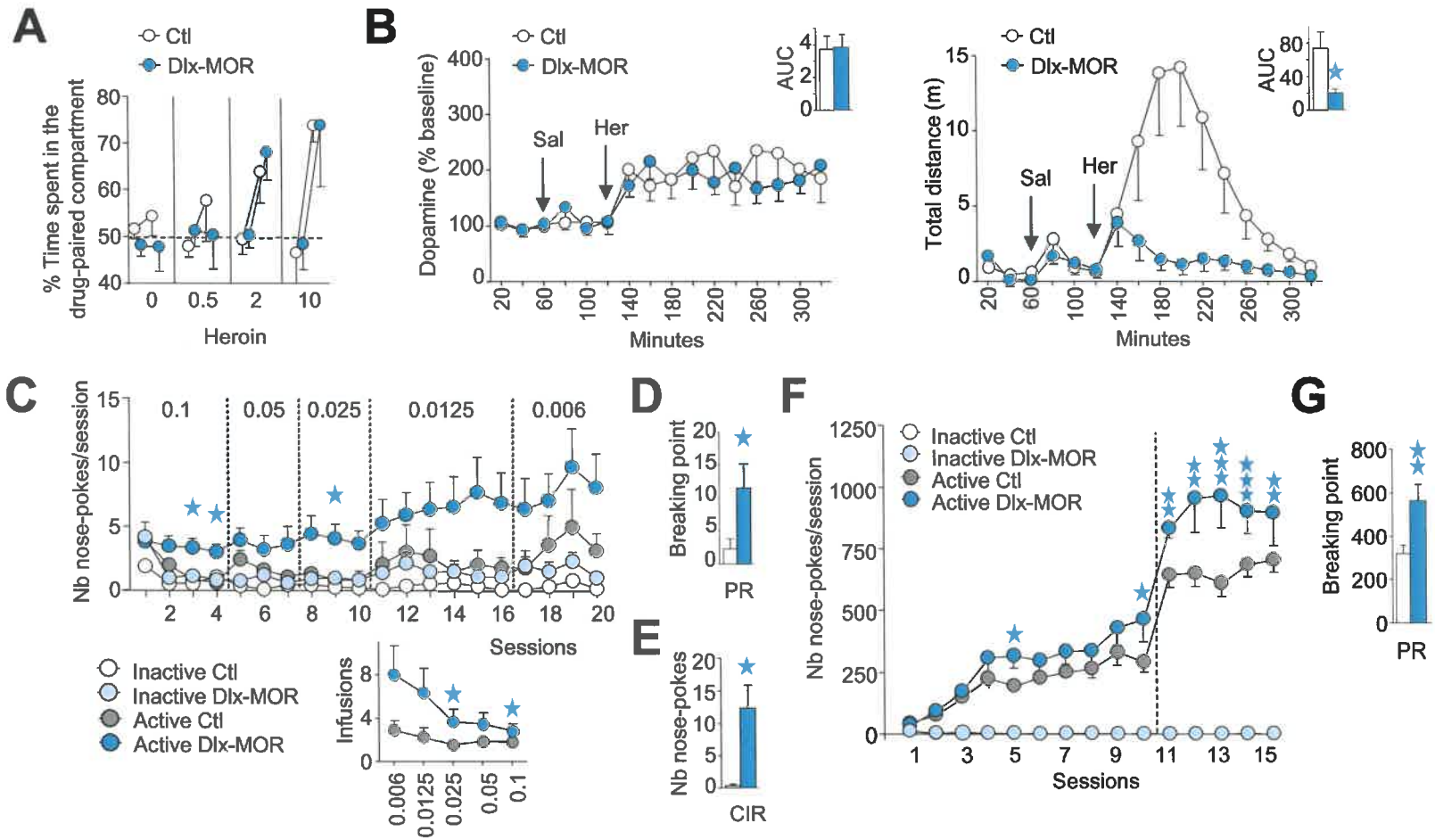

Charbogne et al Figure 4

Supplemental Information

Supplemental Methods and Materials

Drugs. Morphine (hydrochloride, Francopia, Cepia Sanofi, France) and heroin (diacetylmorphine hydrochloride) were provided by Francopia (Cepia Sanofi, France), naloxone (hydrochloride) and amphetamine (D-amphetamine hemisulfate, A-5880) purchased from Sigma-Aldrich, St Louis, USA). All the drugs were dissolved in NaCl 0.9% and administered in a 10 mL/kg volume. For self-administration (SA), heroin was obtained from Ministerio de Sanidad y Consumo (Spain) and delivered intravenously.

Mutant animals.
Generation of Dlx-MOR mice. The floxed *Oprm1* mouse line (*Oprm1*$^{fl/fl}$) harbour exons 2 and 3 of MOR gene flanked by loxP sites, and was described previously by our group (1). These mice were bred with Dlx5/6-Cre mice (obtained from Beat Lutz laboratory, Institute of Physiological Chemistry, Johannes Gutenberg University, Germany) in our vivarium (Institut Clinique de la Souris - Institut de Génétique et de Biologie Moléculaire et Cellulaire, Illkirch, France). Cre positive conditional mutants (Dlx5/6-Cre-*Oprm1*$^{fl/fl}$) animals were obtained (hereafter named Dlx-MOR), and Cre negative animals (*Oprm1*$^{fl/fl}$) were used as Controls (hereafter named Ctl). Total *Oprm1* knockout mice were also produced as negative controls, upon breeding *Oprm1*$^{fl/fl}$ mice with CMV-Cre mice, expressing the Cre recombinase under the control of the cytomegalovirus (CMV, ubiquitous) promoter (2). Genetic background of Dlx-MOR, CMV-MOR and Ctl mice is 63% C57BL/6J-37% 129SvPas.
Genotyping. PCR analysis on genomic DNA was performed in order to genotype mice for presence of 1) Cre recombinase, 2) loxP sites and 3) excision of *Oprm1*. PCR was achieved on DNA from mouse digested digit sample (NaCl 0.2M; Tris-HCl 100 mM pH8.5; EDTA 5mM; SDS 0.2%; proteinase K (Sigma) 10 mg/mL; overnight at 55°C).

The Cre PCR reaction was performed by adding 0.5 µL lysate to 49.5 µL reaction mix (1X PCR buffer (Sigma); $MgCl_2$ (Sigma) 2.5 mM; dNTPs 0.2 mM (Thermo Scientific); TAQ DNA polymerase 2.5 U (Sigma); forward *Cre* primer (5'-GAT CGC TGC CAG GAT ATA CG-3'), reverse *Cre* primer (5'-CAT CGC CAT CTT CCA GCA G-3'), forward *myosin* gene primer (5'-TTA CGT CCA TCG TGG ACA GC-3'), reverse *myosin* gene primer (5'-TGG GCT GGG TGT TAG CCT TA-3') 0.5 µM). PCR temperature cycling parameters were: 94°C 5 min, 30x (94°C 1 min, 62°C 1 min, 72°C 1 min), and 72°C 10 min.

The loxP sites PCR reaction was performed by adding 0.5 µL lysate to 49.5 µL reaction mix (1X PCR buffer GoTaq (Promega); $MgCl_2$ (Sigma) 1 mM; dNTPs 0.4 mM (Thermo Scientific); TAQ DNA polymerase 2.5 U (Promega); forward *mu floxed* gene primer (5'-GTT ACT GGA GAA TCC AGG CCA AGC-3'), reverse *mu floxed* gene primer (5'-TGC TAG AAC CTG CGG AGC CAC A-3') 1 µM). PCR temperature cycling parameters were: 94°C 5 min, 30x (95°C 1 min, 60°C 1 min, 72°C 1 min), and 72°C 10 min.

The *Oprm1* gene excision PCR reaction was performed by adding 0.2 µL lysate to 49.8 µL reaction mix (1X PCR buffer (Sigma); $MgCl_2$ (Sigma) 2.5 mM; dNTPs 0.2 mM (Thermo Scientific); TAQ DNA polymerase 2.5 U (Sigma); forward excision primer (5'-ACC AGT ACA TGG ACT GGA TGT GCC-3'), reverse excision primer (5'-GAG ACA AGG CTC TGA GGA TAG TAA C-3'), forward *myosin* gene primer (5'-TTA CGT CCA TCG TGG ACA GC-3'), reverse *myosin* gene primer (5'-TGG GCT GGG TGT TAG CCT TA-3') 0.5 µM). PCR temperature cycling parameters were: 94°C 5 min, 35x (94°C 30 sec, 61°C 30 sec, 72°C 30 sec), and 72°C 10 min.

mRNA analyses.
In situ hybridization. Wild-type C57B6J male mice were sacrificed, fresh brains included into OCT and cut in a cryostat. The 20-µm thick coronal sections were directly mounted on superfrost slides and kept at -80◦C till processing. *In situ* hybridizations were performed using RNAscope Multiplex Fluorescent Assay (ACD, Advanced Cell Diagnostics, CA, USA). The experiment was conducted in accordance with ACD recommendations for fresh frozen sections. Probes for *Drd1*, *Drd2* and *Oprm1* were revealed using Alexa 488- Atto 550- and Atto-647-labeled probes, respectively, in addition to DAPI staining. Probes were designed by

ACD as follows: *Drd1a*-C2 target region 444-1358, *Drd2*-C3 target region 69-1175, and *Oprm1*-C1 target region 1135-2162. The images were acquired using a slide scanner NanoZoomer 2 HT and fluorescence module L11600-21 (Hamamatsu Photonics, Japan) at 40X magnification and analysed with NDP View software. A 1-mm^2 zone in each hemisphere was selected in one section per animal (n=3) of the NAc (AP +1.1) and three 0.1-mm^2 zones for the DS (AP +1.1). The number of *Oprm1* positive neurons was manually counted using NDP View Ex counter plugin, and colocalization with either *Drd1*, *Drd2* or both was evaluated bilaterally. Results are represented as a percentage of *Oprm1* mRNA positive cells.

Quantitative real-time PCR. Mice were sacrificed by cervical dislocation. Brains were extracted, rinsed in cold 1X PBS (phosphate-buffered saline solution, Sigma) and 1-mm thick slices were cut with a stainless steel coronal brain matrix chilled on ice (Harvard apparatus, Holliston, MA, USA). The different brain regions were collected from 3 to 5 mice per genotype according to the stereotaxic atlas of mouse brain. The dorsal striatum (DS) was bilaterally punched using a 2-mm diameter tissue corer; nucleus accumbens (NAc), ventral tegmental area (VTA), and lateral hypothalamus (LH) were bilaterally punched with a 1.2-mm tissue corer; prefrontal cortex (PCF) and periacqueducal grey (PAG) were centrally punched using a 2-mm diameter tissue corer; habenula (Hb) and dorsal raphe nucleus (DRN) were centrally punched using a 1.2-mm diameter tissue corer; the spinal cord was dissected manually. Samples were immediately frozen on dry ice and kept at -80°C until processing.

Samples were processed to extract total RNA, using TRIzol reagent (Invitrogen, Cergy Pontoise, France) according to manufacturer's instructions. The quality and quantity of RNA was measured with ND-1000 NanoDrop (Thermo Fisher Scientific, Wilmington, USA) spectrophotometer. Reverse transcription of 800 ng to 1 µg total RNA was performed on bilateral pooled brain samples in triplicate, in a 20 µL final volume, with Superscript II kit (Superscript II RT, Invitrogen). Real-time PCR was performed on the resulting cDNA using a Light Cycler 480 apparatus (Roche, Meylan, France) and iQ SYBR Green supermix (Biorad, Marnes-la-Coquette, France). Primers sequences were: CCGAAATGCCAAAATTGTCA (*Oprm1* forward), GGACCCCTGCCTGTATTTTGT (*Oprm1* reverse), GACGGCCAGGTCATCACTAT (*β-actin* forward), CCACCGATCCACACAGAGTA (*β-actin* reverse), TGAGATTCGGGATATGCTGTTG (*arbp* gene "36B4" forward), TTCAATGGTGCCTCTGGAGAT (*arbp* gene "36B4" reverse), TGACACTGGTAAAACAATGCA (*HPRT* forward), GGTCCTTTTCACCAGCAAGCT (*HPRT* reverse), GTCTCCCAGATCGGGCATTT (*drd1* forward), TTCTGGGTTCAGTGCTCCAG (*drd1* reverse), ATCGTCTCGTTCTACGTGCC (*drd2* forward), GTGGGTACAGTTGCCCTTGA (*drd2* reverse), GCTCGTCATGTTTGGCATC (*Oprd1* forward), AAGTACTTGGCGCTCTGGAA (*Oprd1* reverse), TCCTTGGAGGCACCAAAGTCAG (*Oprk1* forward), TGGTGATGCGGCGGAGATTTCG (*Oprk1* reverse), ATGCCGAGATTCTGCTACAGT (*pomc* forward), TCCAGCGAGAGGTCGAGTTT (*pomc* reverse), CGACATCAATTTCCTGGCGT (*penk* forward), AGATCCTTGCAGGTCTCCCA (*penk* reverse), ATGATGAGACGCCATCCTTC (*pdyn* forward), TTAATGAGGGCTGTGGGAAC (*pdyn* reverse). Thermal cycling parameters were 1 min at 95°C followed by 40 amplification cycles of 15 sec at 95°C, 15 sec at 60°C and 30 sec at 72°C. Expression levels were normalized to *β-actin* housekeeping gene levels. Two reference genes (*HPRT*, *arbp*) were tested in each run as an internal control. The $2^{-\Delta\Delta Ct}$ method was used to evaluate differential expression levels (3) of Ctl, Dlx-MOR and CMV-MOR mice. Ctl animals were used as baseline to normalize. A first cohort of Ctl, Dlx-MOR and CMV-MOR mice was used to study the MOR mRNA distribution in a large range of regions (n=2-4); we used 3 to 4 Ctl animals, 3 to 4 Dlx-MOR mice, and 2 to 4 CMV-MOR (total KO for the negative control). The qRT-PCR experiments were done in triplicate, and were run twice. A second cohort, composed of Ctl and Dlx-MOR mice (n=3-4), was used to investigate opioid system and dopamine (DA) receptors mRNA modifications in the NAc and DS. Gene expression (Figure 1B, C and Supplemental Figure S4A) results are expressed relative to Ctl and statistical analysis was performed by a one-sample t test compared to a hypothetical value of 1; Bonferroni correction was used for multiple comparisons.

Autoradiographic binding.

Following decapitation, intact brains were removed, snap frozen at -20°C in isopentane and then stored at -80°C until sectioned. Twenty µm coronal sections were cut in a cryostat (Zeiss Hyrax C 25, Carl Zeiss MicroImaging GmbH, Germany) at 300 µm intervals, from rostral to caudal levels, and thaw-mounted onto gelatine coated ice-cold microscope slides and processed for autoradiography. Adjacent sections were cut for determination of total and non-specific (NSB) binding. Sections were stored at -20°C prior to radioligand binding. MOR binding was carried out as described previously (4) with minor modifications. Briefly, slides were pre-incubated for 30 min in 50 mM Tris-HCl pre-incubation buffer, containing 0.9% w/v NaCl, pH 7.4 at room temperature. The slides were then incubated in 50 mM Tris-HCl buffer, pH 7.4 at room temperature in the presence of 4 nM [^{3}H]DAMGO (specific activity 51.5 Ci/mmol) for 60 min. NSB was determined in the presence of 1 µM naloxone. Incubation was terminated by rapid rinses (3 x 5 min) in ice-cold 50 mM Tris-HCl buffer, pH 7.4 at room temperature and distilled water (3 x 5 min), then rapidly cool-air dried. Following binding, sections were rapidly dried under cold air for 2h, and dried for up to 7 days using anhydrous calcium sulphate (BDH Chemicals, Poole, UK). Adjacent total and non-specific labelled sections were apposed to Kodak BioMax MR-1 film alongside autoradiographic microscale standards of known concentration. [^{3}H]-bound sections were exposed to film with ^{3}H microscale standards for a period of 10 weeks. For development, films were covered with an aqueous solution of 50 % v/v Kodak D19 developer for 3 min. The reaction was stopped by 1 min rinse in distilled water containing a drop of glacial acetic acid. Images were fixed by submersion in Kodak rapid fix solution for 5 min. Films were then rinsed in distilled water and dried overnight in a fume cupboard. Films were analysed by video-based densiometry using an MCID image analyser (Imaging Research, Canada). Fmol/mg tissue equivalents for receptor binding were derived from ^{3}H microscale standards, and the relationship between tissue radioactivity and optical density was calculated using MCID software, with appropriate adjustments to allow for radioactive decay of both the standards and the radioligands. Specific receptor binding was derived by subtraction of NSB from total binding for mu receptors.

For each quantified region, measures were taken from both left and right hemispheres, therefore receptor binding represents a duplicate determination for each brain region and the *n* values listed refer to the number of animals analysed. The following structures were analysed by sampling 5 – 20 times with a box tool: cortex (8 x 8 mm), olfactory tubercle (6 x 6 mm) and hippocampus (5 x 5 mm). All other regions were analysed by free-hand drawing. Brain structures were identified by reference to the mouse atlas of Franklin and Paxinos. Comparison of specific binding in Ctl and Dlx-MOR mice (Figure 1E) was carried out using one-tailed Mann Whitney.

Electrophysiology.

All procedures were performed in accordance with the guidelines of National Institute on Alcohol Abuse and Alcoholism and the Animal Care and Use Committees. Electrophysiology was performed as described previously (5). Briefly, Dlx-MOR mice and littermate controls were anesthetized with isoflurane and transcardially perfused with ice-cold artificial cerebrospinal fluid (aCSF) containing the following (in mM): 124 NaCl, 2.5 KCl, 1.3 MgCl2, 2.5 CaCl2, 1.0 NaH2PO4, 26.2 NaHCO3, 20 D-glucose, 0.4 Ascorbate and 3 Kynurenic Acid. Sagittal slices (220-230 µm) were prepared in ice-cold aCSF using vibratome (Leica). Slices were incubated in warm (33°C) oxygenated aCSF for 30 min and moved to room temperature (22-24°C) until used. Slices containing midbrain were then transferred to the recording chamber that was constantly perfused with oxygenated aCSF at the rate of 1.5-2 mL/min. Midbrain neurons were visualized with a 40x water-immersion objective on an upright microscope (BX51WI, Olympus USA). Whole-cell voltage clamp recording was performed from DA and GABA neurons in VTA using an Axopatch-200B amplifier (Molecular Devices). Patch pipettes (2.0-3.5 MΩ) were filled with an internal solution containing the following (in mM): 57.5 KCl, 57.5 K-methylsulfate, 20 NaCl, 1.5 MgCl2, 5 HEPES, 10 BAPTA, 2 ATP, 0.2 GTP, and 10 phosphocreatine, pH 7.35, 290 mOsM. Physiological identification of DA neurons was based on the presence of D2-autoreceptor-mediated GIRK currents and the rate of spontaneous action potential activity (1-5 Hz) with spike widths ≥1.2 ms (6-9). Identification of GABA neurons was based on the absence of D2-autoreceptor mediated GIRK current, and the range of spontaneous action potential activity

(>10 Hz) with spike widths <1.0 ms. Neurons were voltage clamped at -60 mV and series resistance was monitored throughout the experiment (range; 3-15 MΩ). $GABA_A$ IPSCs were evoked by electrical stimulation using a paired pulse (2 stimuli at 20 Hz) delivered every 20 s via monopolar electrode placed 100-200 µm rostroventral location from the recorded neuron cell body. All recordings were performed in the presence of the glutamate receptor blockers NBQX 5 µM and CPP 5 µM to isolate $GABA_A$ IPSCs.

Data were acquired using pClamp 10 software (sampled at 50 kHz, filtered at 1 kHz). The peak amplitude of $GABA_A$ IPSC was measured using AxoGraphX peak measurement software (Axograph Scientific) after subtracting the baseline; statistical analysis was obtained using unpaired two-tailed t tests if normal distribution of the values (Shapiro-Wilk normality test) or two-tailed Mann Whitney if not normal distribution (Figure 1F, G).

C-Fos protein immunoreactivity.

Animals were weighted and handled for 2 days, and injected daily for 2 days with saline prior to the experiment in order to avoid stress-induced c-Fos expression (10, 11). Mice were deeply anesthetised with ketamine-xylazine (1 g/kg and 100 mg/kg respectively, ip) 2h after a single saline or heroin (10 mg/kg, ip) administration (12), then perfused transcardially with 10 mL ice-cold phosphate buffer (PB, 0.1 M, pH 7.4) followed by 100 mL fresh cold 4% paraformaldehyde (PFA) in 0.1 M PB. Brains were dissected, post-fixated 24 to 48h in 4% PFA and cryoprotected in 30% sucrose (in 1X PB solution) for 48h. Brains were frozen and cut in a cryostat into 50-µm thick coronal sections, collected in 0.1 M PB. Free-floating sections were incubated overnight at room temperature with a primary rabbit polyclonal antibody (Ab-5, Calbiochem, Merck, Darmstadt, Germany, 1:20,000) targeting sequence 4-17 of the Fos protein. The sections were then incubated 2h with a biotinylated goat anti-rabbit IgG secondary antibody (Jackson Immunoresearch, West Baltimore Pike, PA, USA, 1:2,000). C-Fos immunohistochemistry was revealed with a standard avidin-biotin peroxidase method (ABC, Elite Vectastain Kit, Vector Laboratories, Burlingame, CA, USA). Detection of the peroxidase was performed with the chromogen diaminobenzidine (Sigma-Aldrich, Saint-Quentin, France). For a first cohort (n=2 to 4), images were acquired using Hamamatsu Nanozoomer 2-HT (Hamamatsu Photonics, Hamamatsu, Japan) slide scanner. Brightfield 20x magnification images were analysed with NDP View software and Fos-immunoreactive cells were manually counted using NDP View Ex counter plugin. Images from a second cohort (n=2 to 4) were acquired using MIRAX Scan 150 BF/FL (Zeiss, Germany). Comparison of the two acquisition methods showed no difference between cohorts (data not shown) and data were pooled. The number of positive nuclei was counted manually and expressed per mm^2. Scoring was performed bilaterally using 4 to 7 sections per animal, in 7 brain regions (NAc core and shell, dorsomedial, dorsolateral, ventromedial and ventrolateral DS, and VTA) (13). Comparison of neuronal activation of the two genotypes (Ctl and Dlx-MOR) was performed by two-way ANOVA followed by a Student-Newman-Keuls (SNK) *post hoc* analysis (Figure 2A, B).

Resting-state functional Magnetic Resonance Imaging.

All animal experiments were performed in accordance with the guidelines and ethics on animal experimentation established by the German and French laws (ethical allowance 35_9185.81/G-13/15 from Regierungspräsidium Freiburg). Animal preparation, data acquisition and analysis were performed as described previously (14, 15). In brief, resting-state magnetic resonance imaging (BOLD) was performed on two groups of adult male mice – Dlx-MOR (n=10) and the respective wild type Ctl mice (n=12) under medetomidine sedation (sc bolus injection, 0.3 mg per kg body weight in 100 µL 0.9% NaCl-solution right before the scan followed by continuous sc infusion of medetomidine (0.6 mg per kg body weight in 200 µL per hour) during scanning). The physiological parameters including body temperature, respiration rate, blood oxygen saturation and heart rate were continuously monitored to ensure stable and comparable imaging conditions for all animals.

RsfMRI data was collected using single shot Gradient Echo EPI (TE/TR = 10 ms/1700 ms) at a 7 T small bore animal scanner (Biospec 70/20, Bruker, Germany) with a mouse head adapted cryocoil (MRI CryoProbe, Bruker, Germany). Following a shimming protocol, the whole mouse brain (excluding the cerebellum) was covered using 12 axial slices (0.7 mm slice thickness), with a field of view of 1.92 × 1.2 cm^2 and an acquisition matrix of 128 × 80.

This resulted in a planar spatial resolution of 150 × 150 μm^2. 200 volumes were recorded with slice acquisition in interlaced fashion for each run.

The preprocessing pipeline including coregistration with Allen mouse brain atlas (16), creation of brain mask and smoothing with a Gaussian kernel of FWHM 0.4x0.4x1 mm^3 was performed using Matlab and SPM8 (http://www.fil.ion.ucl.ac.uk/spm/).

Spatial Independent Component Analysis (ICA) using ICASSO (Gift - Group ICA of fMRI Toolbox – v.1.3i, http://www.nitrc.org/projects/gift/) was performed on the 22 combined preprocessed Ctl and Dlx-MOR datasets. The analysis (including quality assessment via ICASSO, see (14) for details) revealed 88 out of 100 IC as reliable functional clusters, associated with anatomically well-defined brain areas, as identified via co-registration with Allen brain atlas. These functional clusters were further used as nodes to create the whole brain functional connectivity matrix, for each group separately (Dlx-MOR and Ctl) using partial correlation of the mean time courses of blood oxygen level dependent signal (BOLD) associated to each IC. The resulting matrices were normalized using Fisher's Z transformation. Positive and negative correlations were included in the analysis and the normalized absolute strength and diversity values were calculated for each pair of nodes (17, 18). The functional hubs were determined for both groups, defined as nodes of over average strength and diversity (Figure 2C and Supplemental Figure S2A).

For seed-based Granger Causality, images were re-processed for further seed-based analysis. Briefly, rs-fMRI time series were slice-timing corrected, spatially smoothed (FWHM 0.3 mm), band-pass filtered to a frequency window of 0.01-0.1 Hz (14) and deconvolved (19). Seeds were generated for selected regions following standard size 3 × 3 × 1 voxel (20). Seed locations were based on known neuroanatomical structures from the Paxinos brain atlas (13) and the mean time series of each seed was used for directionality analysis. We then applied Conditional Granger Causality (C-GC) (21), and determined dominant directionality, as the difference in C-GC strength across directions for seed pairs (22). To maximize statistical power, we ran non-parametric permutation test following 100 permutations for each subject (21), and the test was repeated multiple times to ensure consistency and robustness of directional connectivity (Figure 2D and Supplemental Figure S2C).

Cocaine microdialysis.

Mice were anesthetized with a ketamine:xylazine (5:1; 0.10 mL/10 g, ip) solution and placed in a stereotaxic apparatus. Unilateral microdialysis probes (CMA7: 1 mm, CMA Microdialysis, Stockholm, Sweden) were directly implanted vertically in the NAc (AP+1.5; ML±0.8; DV-4.8 mm) from bregma and skull surface according to the coordinates of Paxinos and Franklin (23), and then fixed to the skull with dental cement. Two days after surgery, mice were habituated to the microdialysis environment overnight. The following morning, probes were perfused with a ringer solution (NaCl: 148 mM, KCl: 2.7 mM, CaCl2:1.2 mM and MgCl2: 0.8 mM, pH 6.0) at a constant rate of 1 µL/min during 1 h. Subsequently, 4 dialysates were collected in each mouse in order to determine baseline DA efflux. Then, mice were challenged first with saline followed by two doses of cocaine (10 and 20 mg/kg, ip). Four samples were collected after saline, 4 samples after the dose of 10 mg/kg, 6 samples after the dose of 20 mg/kg, and again 3 samples after saline at 20 min intervals. Dialysates (20 µL) were injected without any purification into an HPLC system that consisted of a pump linked to an automatic injector (Agilent 1100, Palo Alto, USA), a reverse-phase column (Zorbax SB C18, 5 mm, 150 x 4.6 mm, Agilent Technologies, Palo Alto, USA), and a coulometric detector (Coulochem II, ESA Inc., Chelmsford, USA) with a 5011A analytical cell. DA was quantified as previously described (24). At the end of the experiments, mice were sacrificed and brains cut using a cryostat. Serial coronal sections (20 µm) were then processed with Cresyl Violet (Sigma-Aldrich, Madrid, Spain). Only those mice with correct probe placements were used in the study. For microdialysis experiments (Supplemental Figure S4C), statistical analyses were performed using two-way ANOVA with repeated measures.

Heroin microdialysis.

Mice were deeply anesthetized with isoflurane and stereotaxically implanted with an 11 mm stainless steel guide cannula (C311G, below pedestal, HRS Scientific, Canada) into the NAc

(AP+1.70; ML±0.9; DV-3.3 mm). Mice were allowed to recover for a week prior to the dialysis experiment and single-housed. On the day of testing, a microdialysis probe [in-house, see (25)] was inserted into the guide cannula. Computer-controlled microinfusion pumps were used to deliver the aCSF (in mM: 126 NaCl, 3.0 KCl, 1.3 $MgCl_2$, 2.3 $CaCl_2$, 1.2 NaH_2PO_4, 26.0 $NaHCO_3$, 0.2 L-ascorbic acid) at a rate of 1µL/min during a 2h period of stabilization. Dialysates were subsequently collected every 20 min for 60 min to establish baseline and then for 60 min after saline injection and finally 200 min after heroin (10 mg/kg, ip) injection and immediately transferred into a tube containing 1µL of 0.25 M perchloric acid. Horizontal activity of Ctl and Dlx-MOR mice was assessed concomitantly, in individual cages (VersaMax, Omnitech Electronics Inc., USA) equipped with photobeams. Dialysate samples were kept at 4◦C until analyzed using HPLC coupled to electrochemical detection. At the end of the experiments, mice were sacrificed and brains cut using a cryostat. Serial coronal sections (20 µm) were then processed with Cresyl Violet (Sigma-Aldrich, Madrid, Spain). Only those mice with correct probe placements were used in the study. For microdialysis experiments (Figure 4B and Supplemental Figure S4C) and associated locomotor activity, statistical analyses were performed using two-way ANOVA with repeated measures. DA AUC was analysed by two-tailed Mann Whitney (Shapiro-Wilk: distribution not normal) and locomotion AUC by two-tailed unpaired t test (Shapiro-Wilk: normal distribution).

Behavior.
All experiments were carried out according to the recommendations of the IASP (26) and the European Communities Council Directive of September 22, 2010 (directive 2010/63/UE). Animal protocols were approved by the local bioethics committee (Comité d'Éthique pour l'Expérimentation Animale, Institut Clinique de la Souris - Institut de Génétique et de Biologie Moléculaire et Cellulaire, Illkirch, France). For most experiments, animals were group-housed (2 to 5) in a room maintained at 21±2°C and 45±5% humidity, with a 12h light-dark cycle (lights on at 7.00 h, off at 19.00 h). All testing procedures were carried during the light phase. Food and water were available *ad libitum*. Experiments were performed using both male and female mice 8/20-week old at the beginning of the study, habituated to the experimental environment and handled for 2 days before behavioral testing. Experimental room light was set at 15 lux. All behavioral testing was performed with the observer blind to the genotype or treatment. Group assignment was pseudo-randomized. DA microdialysis experiments were carried out with 8/15-week old animals and only males were used. For self-administration (SA) procedures experiments were carried out with 8/18-week old males and only males were used. Mice were housed individually in controlled laboratory conditions with the temperature maintained at 21±1 ºC and humidity at 55±10%. Mice were tested during the first hours of the dark phase of a reversed light/dark cycle (lights off at 8.00 h and on at 20.00 h). For experiments of operant conditioning maintained by chocolate, mice were food-deprived (85 % of the initial weight) and water was available *ad libitum*. Animal procedures were conducted in strict accordance with the guidelines of the European Communities Directive 86/609/EEC regulating animal research and were approved by the local ethical committee (CEEA-PRBB, Barcelona, Spain). Outliers were excluded using ESD method (extreme studentized deviate).

Nociception. TI-TF: Analgesic effects of morphine on thermal nociception were assessed using tail immersion (TI) and tail flick (TF) tests. Mice received ip injections of cumulative doses of morphine (0, 2, 4, 6 and 10 mg/kg) every 30 minutes. All the 3 tests were done successively, with one-minute interval between each test (TI 52°C, then TI 54°C and finally TF). Mice were restrained in a tube during the 3 tests. For TI tests (27), the bottom half of the mouse tail was dipped in a 52°C/54°C water bath and the latency for tail withdrawal was measured. For the TF test, the mouse tail was placed on a heating laser (intensity setting 40, radial heat, Tail Flick apparatus, DL Instrument International) and the latency for tail flick was measured. To avoid tissue damage, a cut-off was determined according to basal nociceptive threshold (respectively 20, 15 and 15 sec). For the hot plate test, animals were placed on a 54◦C hot plate (Bioseb, France), surrounded by a Plexiglas cylinder, 30 minutes after morphine injection (0, 2 or 5 mg/kg, ip) (27). The latency to show first signs of discomfort (forepaw lick, hindpaw lick and jump) was measured. Jump is defined as no contact of the 4 paws with the plate and a 240-sec cut-off time was applied. TI and TF experiments were

analysed by a two-way ANOVA with repeated measures with morphine doses as within factor (Figure 3A-B), and hot plate test by a two-way ANOVA (Figure 3C), all followed by Bonferroni's multiple comparison test (treatment effect compared to saline group).

Physical dependence and withdrawal. Mice received chronic escalating morphine treatment during 6 days (10, 20, 40, 60, 80 and 100 mg/kg, ip see (27). The twice daily injections were separated by 8h min. On day 7, a last 100 mg/kg morphine dose was injected 2 hours prior testing. In a room lighted at 15 lux, mice were placed in Plexiglas observation boxes (30 x 15 x 15cm) and basal activity was observed during 5 min. Withdrawal was precipitated by a naloxone injection (1 mg/kg, sc) for both morphine and vehicle-treated animals, and mice were placed back into the observation boxes for 20 min. Number of paw tremors, jumps, head shakes, wet dog shakes and sniffing was counted; ptosis, teeth chattering and piloerection presence was evaluated during each 5-min period. A general withdrawal score was calculated, with a coefficient for each component (jumping x 0.8; wet dog shakes x 1; paw tremor x 0.35; sniffing x 0.5; ptosis x 1.5; teeth chattering x 1.5; body tremor x 1.5; piloerection x 1.5) (28). Additional signs were scored to complete the observation (activity, grooming, rearing). Withdrawal scoring was analyzed by a two-way ANOVA (Figure 3D) followed by Bonferroni's multiple comparison test (treatment effect compared to saline group).

Locomotor activity. Mice locomotion was assessed in Plexiglas boxes (21 × 11 × 17 cm) placed over an infrared platform, light intensity of the room set at 15 lux (29). Animal traveling distances were analyzed and recorded via an automated tracking system equipped with an infrared-sensitive camera (Videotrack; View Point, Lyon, France). Speed sensitivity was set at 6 cm/sec. Mice were placed individually in the activity boxes for a 60 min-habituation period to reach a stable basal activity. Then, mice received injection of vehicle, heroin (0.5, 2, 4, 6, 8 or 10 mg/kg, ip) or amphetamine (2.5 or 5 mg/kg, ip) and were placed back in the same boxes. Drug-induced locomotor effects were recorder for further 120 min. Two-way ANOVA was used, followed by Bonferroni's multiple comparison test (Figure 3E and Supplemental Figure S4B).

Locomotor sensitization. Mice locomotor sensitization to heroin was assessed in the same conditions as acute heroin locomotion recordings. Briefly, during the first session, mice basal locomotion was measured during a 60 min-habituation period. Mice received then a heroin injection (0 or 10 mg/kg, ip) and were placed back in the locomotor boxes for 2h. The same experiment is conducted in the same mice every 4 days, to produce a locomotor sensitization during 5 sessions (day 1 to day 17). Data were analysed using a three-way ANOVA with repeated measures with sessions as within factor, followed by SNK *post hoc* test (Figure 3F).

Bar test. Animals received injection of either saline or heroin (2, 6 or 10 mg/kg, ip) 30 min prior to the test (30). Muscular rigidity is assessed by placing the forepaws of the mice on a horizontal bar (0.4 cm diameter, 4.5 cm above the surface). Latency for the mouse to withdraw its forepaws is measured, using a cut-off time of 2 min. Two-way ANOVA was used, followed by Bonferroni's multiple comparison test (Figure 3G).

Conditioned place preference. CPP boxes (Imétronic, Pessac, France) were composed of 2 compartments (15.5 x 16.5 x 20 cm) separated by a corridor (6 x 16.5 x 20 cm) (31). The 2 boxes had the same size and distinct shape and floor texture. Dim light was used to diminish stress level (30 lux). Automated movement detection was recorded by infrared beams (Place Preference, Imétronic). Procedure consisted of pre-conditioning, conditioning and test phases. During a 20-min pre-conditioning, mice were allowed to freely explore the entire apparatus. Time spent in both boxes is calculated. Animals spending more than 67% in one compartment are excluded. According to pre-conditioning results, a drug-paired box is assigned to each mouse to balance groups in an unbiased procedure. Day 2 to 4, on the morning, mice received either saline or heroin (0.5, 2 or 10 mg/kg, sc) injection and are confined in the drug-paired compartment for 20 min. Seven hours later, during the 20-min afternoon conditioning session, mice were all injected with saline solution and confined in the other chamber. Test occurred on day 5. Mice were free to explore the apparatus during 20

min and time spent in both compartments was recorded. CPP experiments were analysed using three-way ANOVA (Figure 4A).

Self-administration procedures.

a) Heroin self-administration

Apparatus. The operant SA apparatus has been previously described elsewhere (32).

Surgery. The operant SA surgery has been previously described elsewhere (32), with small changes. Ketamine hydrochloride (100 mg/kg, Imalgène 1000; Rhône Mérieux, Lyon, France) and xylazine hydrochloride (20 mg/kg) (Sigma, Madrid, Spain) were mixed and dissolved in ethanol (5 %) and distilled water (95 %). This anaesthetic mixture was administered ip in an injection volume of 20 mL/kg of body weight. Thiopental sodium (5 mg/mL, Braun Medical S.A, Barcelona, Spain) was dissolved in distilled water and delivered by infusion of 0.1 mL through the iv catheter. The catheter was flushed daily with a heparinised saline (30 USP units/mL). The patency of intravenous catheters was evaluated after the PR session and whenever drug SA behavior appeared to deviate dramatically from that observed previously by infusion of 0.1 mL thiopental sodium (5 mg/mL) through the catheter. If prominent signs of anaesthesia were not apparent within 3 s of the infusion, the mouse was removed from the experiment. The success rate for maintaining patency of the catheter (mean of duration of 11 days) until the end of the heroin SA training was 90%. The verification of the catheter patency was not necessary for the extinction and reinstatement phases since heroin was not available.

Acquisition of operant responding maintained by heroin. Heroin SA sessions were performed in accordance to protocols previously described (32-35). Acquisition of operant conditioning maintained by heroin was performed by using different doses in decreasing order (0.1, 0.05, 0.025, 0.0125 and 0.006 mg/kg per injection, i.v.) delivered in 23.5 µL over 2 sec. Mice were given 1-h daily SA sessions during 20 consecutive days under fixed ratio (FR) 1 schedule of reinforcement. Nose-poking on the active hole resulted in the delivery of a reinforcer (heroin), while nose-poking on the inactive hole had no consequences. The side of active and inactive hole was counterbalanced between animals. The house light was on at the beginning of the session for 3 sec and off during the remaining time of the session. No extra houselight was turned on during session. Each daily session started with a priming injection of the drug. At the dose of 0.0125 mg/kg per injection iv, animals were tested in a progressive ratio (PR) schedule where the response requirement to earn the reinforcer escalated according to the following series: 1-2-3-5-12-18-27-40-60-90-135-200-300-450-675-1000. The maximum duration of the PR session was 3 h or until mice did not respond on any hole within 1 h, and was performed only once. Mice were feed *ad libitum* during the whole experiment. The stimuli light together with the pump noise (environmental cues) signaled delivery of the heroin infusion. The timeout period after infusion delivery was 10 sec. During this 10 sec period, the cue light was off and no reward was provided after nose-poking on the active hole. Responses on the inactive hole and all the responses elicited during the 10 s timeout period were also recorded. The session was terminated after 50 reinforcers were delivered or after one hour, whichever occurred first. As previously described (32-35), the criteria for SA behavior was achieved when all of the following conditions were met: 1) mice maintained a stable responding with less than 20 % deviation from the mean of the total number of reinforcers earned in three consecutive sessions (80 % of stability); 2) at least 75 % responding on the active hole, and 3) a minimum of 5 reinforcers per session. After each session, mice were returned to their home-cages. Each chamber was cleaned at the end of each session to prevent the presence of odor of the previous mouse. On day 21, after operant conditioning maintained by heroin at the dose of 0.006 mg/kg/infusion mice were moved from the heroin SA/training phase to the extinction phase. Analysis of the data during the acquisition phase of operant conditioning maintained by heroin was conducted using three-way ANOVA of repeated measures with day and hole (active/inactive) as within-subjects factors and genotype as between-subjects factor (Figure 4C, Table 1). *Post hoc* analysis (Newman-Keuls) was also performed when required. Three-way ANOVA was performed separately for each dose. Data of the breaking point achieved during the PR sessions were analysed with two-tailed Mann Whitney (Shapiro-Wilk: distribution not normal) (Figure 4D).

Extinction of operant responding maintained by heroin. The experimental conditions during the extinction phase were similar to the acquisition of operant responding sessions except that heroin was not available and stimuli lights (environmental cues) were not presented after nose-poking in the active hole. Mice were given 1-h daily sessions (7 days per week) until reaching the extinction criterion. The criterion for extinction was achieved when mice made during 3 consecutive sessions a mean number of nose-poking in the active hole of less than 30 % of the responses obtained during the mean of the three days of achievement of the acquisition criteria of heroin SA training. All animals were run during 10 consecutive daily sessions. Then after, all mice were test under reinstatement induced by cue.

Cue-induced reinstatement. The presentation of conditioned environmental cue was performed to evaluate the reinstatement of heroin-seeking behavior. Test for cue-induced reinstatement was conducted under the same conditions used in the training phase except that heroin was not available. Each nose-poke in the active hole led to the presentation of both stimuli lights for 2 sec. The reinstatement criterion was achieved when nose-pokes in the active hole were double than nose-pokes in the active hole during the 3 consecutive days that mice acquired extinction criteria or a minimum of 10 nose-pokes in the active hole. Data of the cue-induced reinstatement were analysed with two-tailed Mann Whitney (Shapiro-Wilk: distribution not normal) (Figure 4E).

b) Food self-administration.

Apparatus and acquisition of operant responding maintained by chocolate. The protocol has been previously described in (29). Analysis of the data during the acquisition phase of operant conditioning maintained by chocolate was conducted using three-way ANOVA of repeated measures with day and hole (active/inactive) as within-subjects factors and genotype as between-subjects factor (Figure 4F, Table 2). *Post-hoc* analysis (Newman-Keuls) was also performed when required. Three-way ANOVA was performed separately for FR1 and FR5. Data of the breaking point achieved during the PR sessions were analysed with two-tailed Mann Whitney (Shapiro-Wilk: distribution not normal) (Figure 4G).

Statistical analyses

Data are presented as mean ± standard error (SEM). Statistical significance was achieved by $p<0.05$. Statistical analyses were performed using the Statistical Package for Social Science program (SPSS, SPSS Inc., Chicago, IL, USA) for three-way ANOVA and Prism6 (GraphPad Software) for the other tests. For all the analyses, the normal distribution of the values was assessed before any other statistical analysis; we then used parametric testing for a normal distribution and non parametric comparison tests when the distribution of values was not normal.

Supplemental Results

Dlx-MOR mice show intact morphine-induced analgesia and physical dependence

We examined the phenotypic consequences of the conditional MOR knockout on nociception responses to acute morphine administration. To do so, we investigated morphine analgesia in the tail immersion test at 52°C (Figure 3A) and 54°C (not shown) and tail flick test (Figure 3B), classical thermal nociception paradigms used to assess acute analgesic effects of opiates. We compared the analgesic properties of four doses of morphine in Ctl and Dlx-MOR animals. Two-way repeated measures ANOVA of tail immersion (52 and 54°C) and tail flick tests revealed a treatment effect ($F_{5,110}=122.6$; $p<0.001$; $F_{5,110}=149.7$; $p<0.001$; $F_{5,110}=91.30$; $p<0.001$ respectively), but neither genotype effect ($F_{1,22}=0.20$; $p=0.66$; $F_{1,22}=0.157$; $p=0.70$; $F_{1,22}=0.027$; $p=0.87$) nor interaction genotype X treatment ($F_{5,110}=0.28$; $p=0.92$; $F_{5,110}=0.25$; $p=0.94$; $F_{5,110}=0.12$; $p=0.99$) (Figure 3A, B). Planned t-tests comparing the effect of morphine doses to baseline showed that morphine treatment was effective from 4 mg/kg ($p<0.001$) in the three behavioral tests for each genotype. Similarly, 2-way ANOVA revealed a treatment effect in the hot plate test in latency to lick forepaws ($F_{2,35}=13.44$; $p<0.001$), latency to lick the hindpaws (flinching) ($F_{2,32}=18.71$; $p<0.001$) and latency to jump ($F_{2,35}=47.73$; $p<0.001$) (Figure 3C). Neither genotype nor interaction genotype X treatment effects were detected in the hot plate test for the 3 criteria measured: latency to lick forepaws

($F_{1,35}$=1.21; p=0.28; $F_{2,35}$=0.39; p=0.68), flinching latency ($F_{1,32}$=0.038; p=0.85; $F_{2,32}$=0.32; p=0.73) and latency to jump ($F_{1,35}$=0.36; p=0.55; $F_{2,35}$=0.096; p=0.91). Thus, selective inactivation of the MOR in forebrain GABAergic neurons does not alter analgesic properties of morphine.

We also determined whether the conditional deletion of MORs alters the development of physical dependence to chronic morphine treatment, a syndrome that engages broad adaptations throughout brain circuits. We induced physical dependence to morphine by repeated injections of ascending doses of morphine (10–100 mg/kg), twice daily over 6 days. Two hours after the last morphine or saline injection, a single naloxone dose (1 mg/kg, sc) was administered and withdrawal signs were scored. A global withdrawal score was calculated [adapted from (28)] for Ctl and mutants (Figure 3D). Two-way ANOVA of the global withdrawal score revealed a morphine effect ($F_{1,45}$=104.0, p<0.001) that is not different between genotypes ($F_{1,45}$=0.17, p=0.68, interaction genotype X treatment $F_{1,45}$=0.31, p=0.58). No sign of opiate withdrawal was observed during the 5-minute observation session before naloxone administration (data not shown). All the individual signs of withdrawal scored were similar in both genotypes (Supplemental Figure S3). Deletion of MOR in forebrain GABAergic neurons did not alter the physical dependence induced by chronic morphine administration.

Dlx-MOR mice show intact integrity and functionality of the DA system

To explore the integrity of the DA system, we first determined D1 (*Drd1)* and D2 (*Drd2*) receptors mRNA expression from Ctl and Dlx-MOR mice in NAc (left) and DS (right) (Supplemental Figure S4A) by qRT-PCR, as in Figure 1. The analysis of one-sample t test compared to a hypothetical value of 1 revealed no changes in DA receptor transcripts expression in Dlx-MOR animals in the NAc (*Drd1* t_3=0.033, p=0.98; *Drd2* t_3=0.76, p=0.50) and DS (*Drd1* t_3=0.85, p=0.46; *Drd2* t_3=0.53, p=0.63). Similarly, expression level of the *Drd2* mRNA in the VTA, encoding presynaptic D2 receptors in the striatum, was unchanged (not shown).

To explore the functionality of the DA system, we next examined the effect of amphetamine in locomotor activity (Supplemental Figure S4B). Treatment effect was significant ($F_{2,41}$=26.37, p<0.001, 2-way ANOVA), but there was neither genotype effect ($F_{1,41}$=0.34, p=0.56) nor genotype X treatment interaction ($F_{2,41}$=0.54, p=0.59). Bonferroni *post hoc* analysis revealed a difference between 5 mg/kg amphetamine administration and the other doses (p<0.001). We then explored DA release after cocaine (10 and 20 mg/kg) administration in both genotypes (Supplemental Figure S4C). The analysis of two-way repeated measures ANOVA revealed that cocaine dose-dependently increases NAc extracellular DA levels in Dlx-MOR and Ctl mice (time effect, $F_{19,418}$=36.30, p<0.001) with no genotype effect ($F_{1,22}$=0.86, p=0.36) or interaction ($F_{19,418}$=0.82, p=0.69).

Supplemental References

1. Weibel R, Reiss D, Karchewski L, Gardon O, Matifas A, Filliol D, et al. (2013): Mu opioid receptors on primary afferent nav1.8 neurons contribute to opiate-induced analgesia: insight from conditional knockout mice. *PLoS One*. 8:e74706.
2. Metzger D, Chambon P (2001): Site- and time-specific gene targeting in the mouse. *Methods*. 24:71-80.
3. Livak KJ, Schmittgen TD (2001): Analysis of relative gene expression data using real-time quantitative PCR and the 2(-Delta Delta C(T)) Method. *Methods*. 25:402-408.
4. Slowe SJ, Simonin F, Kieffer B, Kitchen I (1999): Quantitative autoradiography of mu-,delta- and kappa1 opioid receptors in kappa-opioid receptor knockout mice. *Brain Res*. 818:335-345.
5. Matsui A, Jarvie BC, Robinson BG, Hentges ST, Williams JT (2014): Separate GABA afferents to dopamine neurons mediate acute action of opioids, development of tolerance, and expression of withdrawal. *Neuron*. 82:1346-1356.
6. Chieng B, Azriel Y, Mohammadi S, Christie MJ (2011): Distinct cellular properties of identified dopaminergic and GABAergic neurons in the mouse ventral tegmental area. *J Physiol*. 589:3775-3787.

7. Ford CP, Mark GP, Williams JT (2006): Properties and opioid inhibition of mesolimbic dopamine neurons vary according to target location. *J Neurosci*. 26:2788-2797.
8. Li W, Doyon WM, Dani JA (2012): Quantitative unit classification of ventral tegmental area neurons in vivo. *J Neurophysiol*. 107:2808-2820.
9. Ungless MA, Magill PJ, Bolam JP (2004): Uniform inhibition of dopamine neurons in the ventral tegmental area by aversive stimuli. *Science*. 303:2040-2042.
10. Reichmann F, Painsipp E, Holzer P (2013): Environmental enrichment and gut inflammation modify stress-induced c-Fos expression in the mouse corticolimbic system. *PLoS One*. 8:e54811.
11. Ziolkowska B, Korostynski M, Piechota M, Kubik J, Przewlocki R (2012): Effects of morphine on immediate-early gene expression in the striatum of C57BL/6J and DBA/2J mice. *Pharmacol Rep*. 64:1091-1104.
12. Bontempi B, Sharp FR (1997): Systemic morphine-induced Fos protein in the rat striatum and nucleus accumbens is regulated by mu opioid receptors in the substantia nigra and ventral tegmental area. *J Neurosci*. 17:8596-8612.
13. **Paxinos G FK (2004): The Mouse Brain in Stereotaxic Coordinates**. ***Gulf Professional Publishing***.
14. Mechling AE, Hubner NS, Lee HL, Hennig J, von Elverfeldt D, Harsan LA (2014): Fine-grained mapping of mouse brain functional connectivity with resting-state fMRI. *Neuroimage*. 96:203-215.
15. Mechling AE AT, Lee H-L, Bienert T, Reisert M, Ben Hamida S, Darcq E, Hennig J, v. Elverfeldt D, Kieffer BL* and Harsan L-AA* (*in press*): Deletion of the mu opioid receptor gene in mice reshapes the reward-aversion connectome. *Proceedings of the National Academy of Sciences*.
16. Lein ES, Hawrylycz MJ, Ao N, Ayres M, Bensinger A, Bernard A, et al. (2007): Genome-wide atlas of gene expression in the adult mouse brain. *Nature*. 445:168-176.
17. Newman ME (2006): Modularity and community structure in networks. *Proc Natl Acad Sci U S A*. 103:8577-8582.
18. Rubinov M, Sporns O (2010): Complex network measures of brain connectivity: uses and interpretations. *Neuroimage*. 52:1059-1069.
19. Wu GR, Liao W, Stramaglia S, Ding JR, Chen H, Marinazzo D (2013): A blind deconvolution approach to recover effective connectivity brain networks from resting state fMRI data. *Med Image Anal*. 17:365-374.
20. Sforazzini F, Schwarz AJ, Galbusera A, Bifone A, Gozzi A (2014): Distributed BOLD and CBV-weighted resting-state networks in the mouse brain. *Neuroimage*. 87:403-415.
21. Barnett L, Seth AK (2014): The MVGC multivariate Granger causality toolbox: a new approach to Granger-causal inference. *J Neurosci Methods*. 223:50-68.
22. Roebroeck A, Formisano E, Goebel R (2005): Mapping directed influence over the brain using Granger causality and fMRI. *Neuroimage*. 25:230-242.
23. Paxinos G, Franklin K (2004): *The mouse brain in stereotaxic coordinates*. San Diego: Elseiver Academic.
24. Robledo P, Mendizabal V, Ortuno J, de la Torre R, Kieffer BL, Maldonado R (2004): The rewarding properties of MDMA are preserved in mice lacking mu-opioid receptors. *Eur J Neurosci*. 20:853-858.
25. Lupinsky D, Moquin L, Gratton A (2010): Interhemispheric regulation of the medial prefrontal cortical glutamate stress response in rats. *J Neurosci*. 30:7624-7633.
26. Zimmermann M (1983): Ethical guidelines for investigations of experimental pain in conscious animals. *Pain*. 16:109-110.
27. Matthes HW, Maldonado R, Simonin F, Valverde O, Slowe S, Kitchen I, et al. (1996): Loss of morphine-induced analgesia, reward effect and withdrawal symptoms in mice lacking the mu-opioid-receptor gene. *Nature*. 383:819-823.
28. Berrendero F, Castane A, Ledent C, Parmentier M, Maldonado R, Valverde O (2003): Increase of morphine withdrawal in mice lacking A2a receptors and no changes in CB1/A2a double knockout mice. *Eur J Neurosci*. 17:315-324.

29. Chu Sin Chung P, Keyworth HL, Martin-Garcia E, Charbogne P, Darcq E, Bailey A, et al. (2015): A novel anxiogenic role for the delta opioid receptor expressed in GABAergic forebrain neurons. *Biol Psychiatry*. 77:404-415.
30. Tzschentke TM, Schmidt WJ (1996): Morphine-induced catalepsy is augmented by NMDA receptor antagonists, but is partially attenuated by an AMPA receptor antagonist. *Eur J Pharmacol*. 295:137-146.
31. Le Merrer J, Plaza-Zabala A, Del Boca C, Matifas A, Maldonado R, Kieffer BL (2011): Deletion of the delta opioid receptor gene impairs place conditioning but preserves morphine reinforcement. *Biol Psychiatry*. 69:700-703.
32. Martin-Garcia E, Barbano MF, Galeote L, Maldonado R (2009): New operant model of nicotine-seeking behaviour in mice. *Int J Neuropsychopharmacol*. 12:343-356.
33. Burokas A, Gutierrez-Cuesta J, Martin-Garcia E, Maldonado R (2012): Operant model of frustrated expected reward in mice. *Addict Biol*. 17:770-782.
34. Soria G, Barbano MF, Maldonado R, Valverde O (2008): A reliable method to study cue-, priming-, and stress-induced reinstatement of cocaine self-administration in mice. *Psychopharmacology (Berl)*. 199:593-603.
35. Soria G, Mendizabal V, Tourino C, Robledo P, Ledent C, Parmentier M, et al. (2005): Lack of CB1 cannabinoid receptor impairs cocaine self-administration. *Neuropsychopharmacology*. 30:1670-1680.

Supplemental Figures

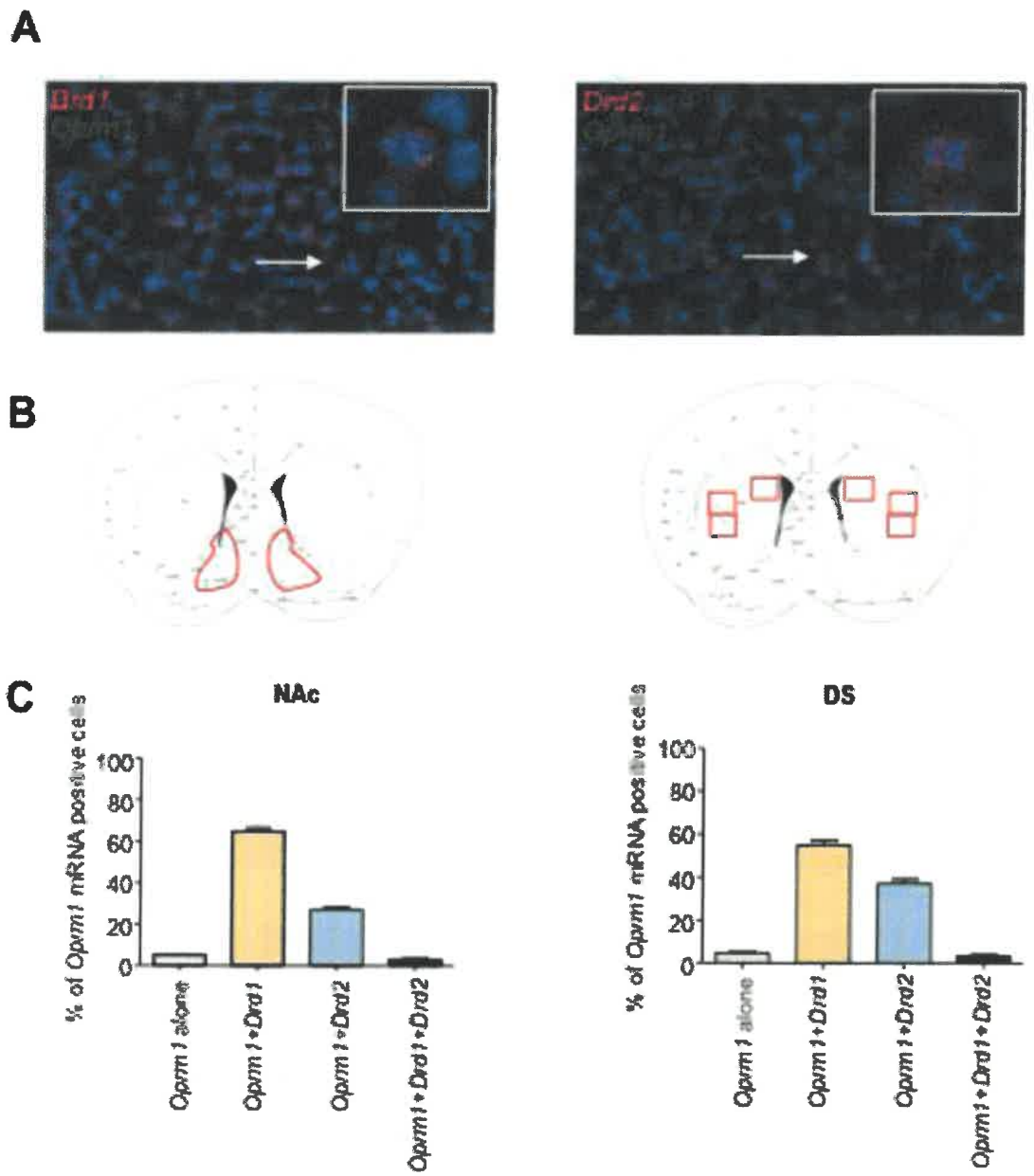

Charbogne et al Supplemental Figure S1

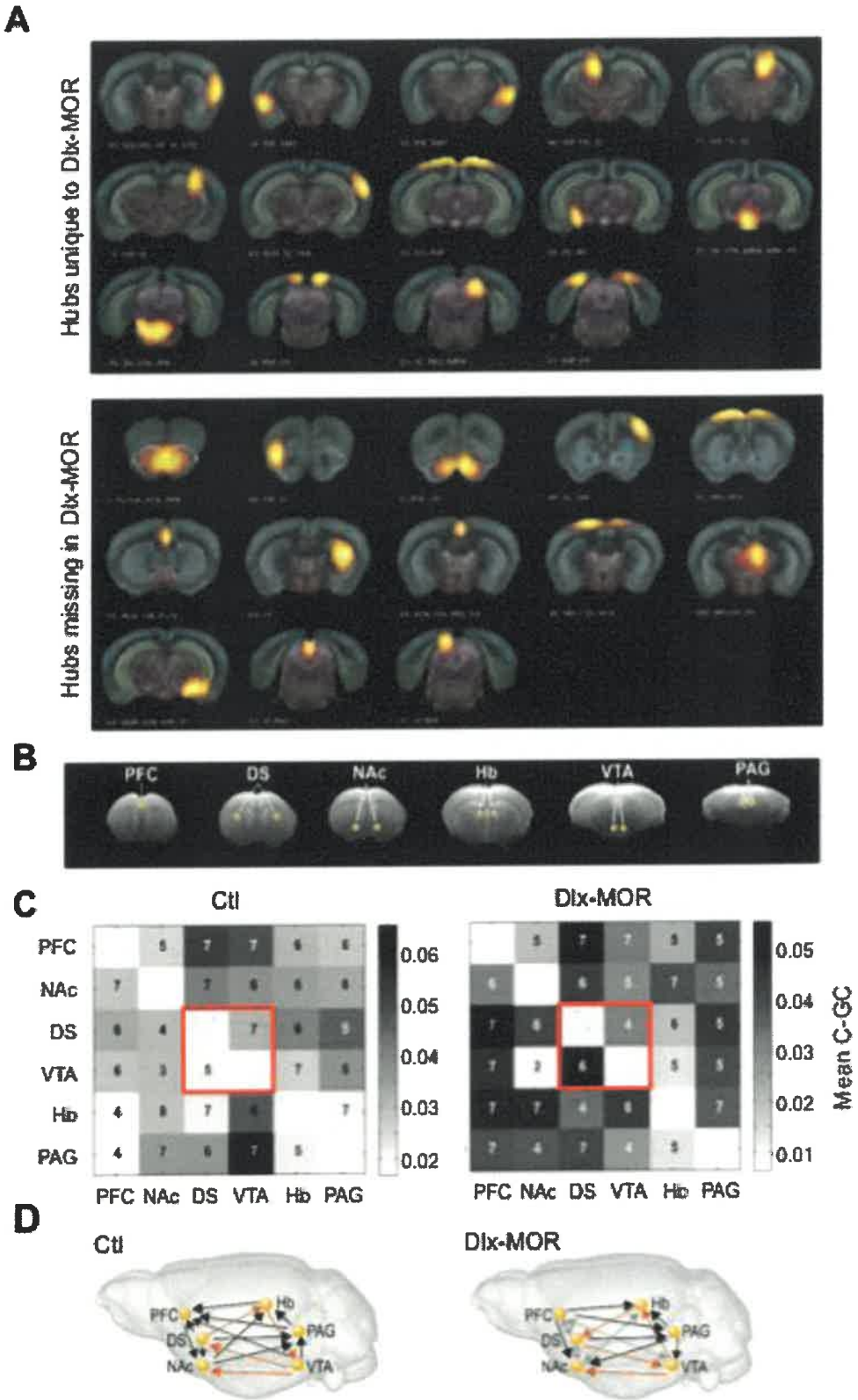

Charbogne et al Supplemental Figure S2

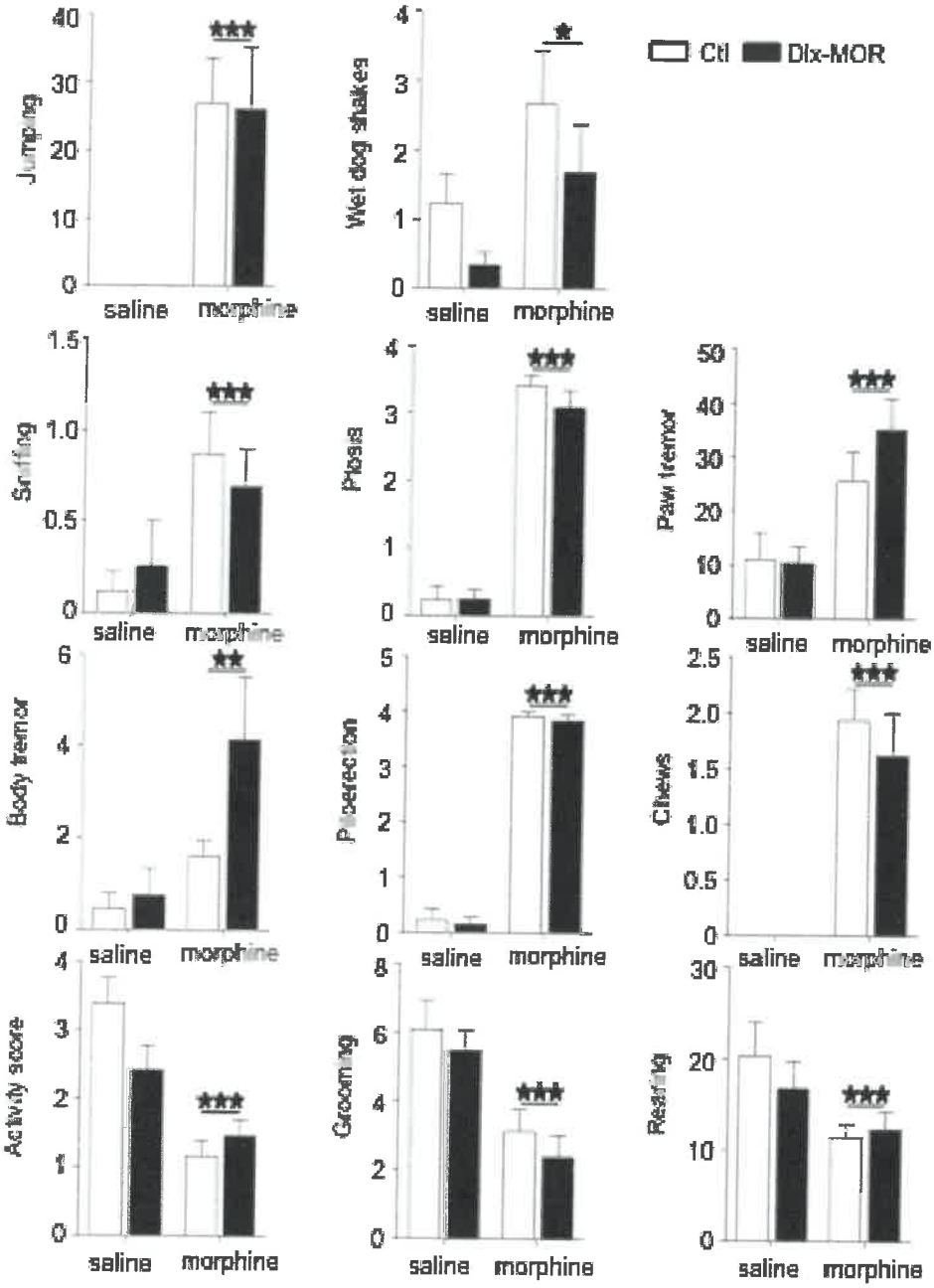

Charbogne et al Supplemental Figure S3

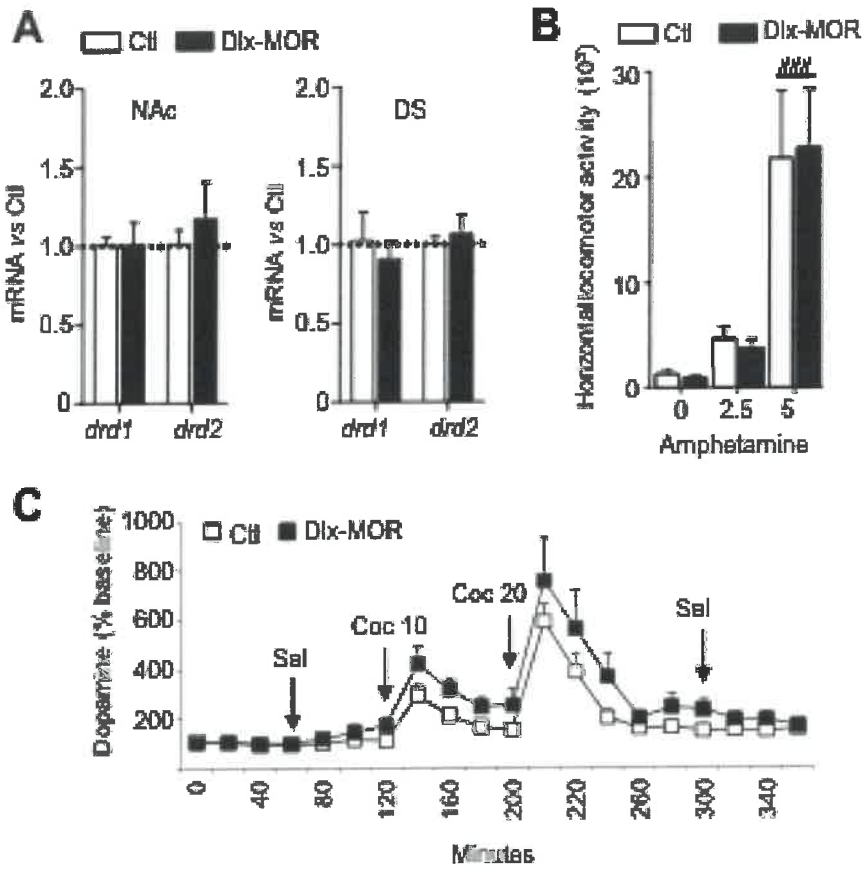

Charbogne et al Supplemental Figure S4

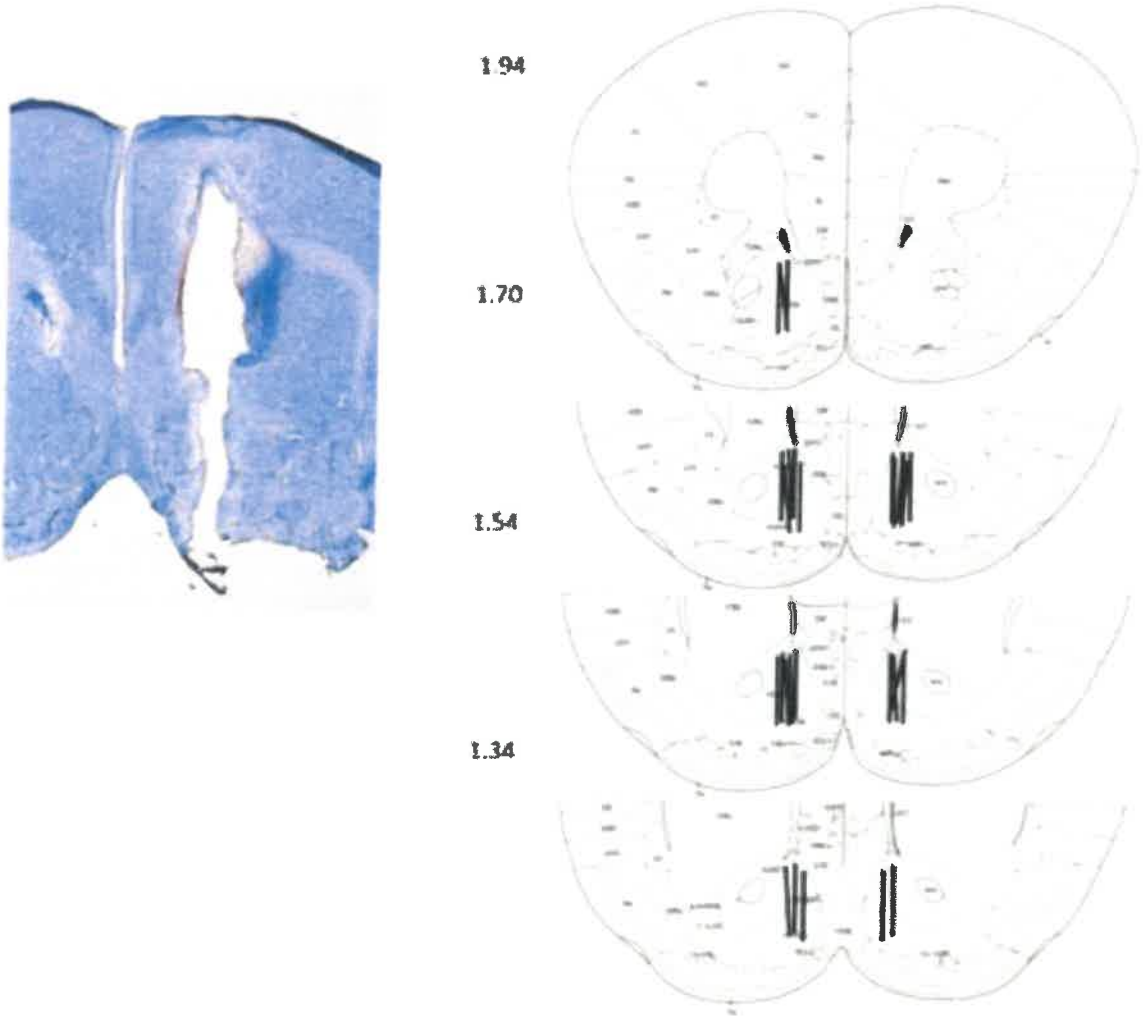

Charbogne et al Supplemental Figure S5

Supplemental Legends

Supplemental Figure S1. *Oprm1* transcript mainly co-localizes with *Drd1* and *Drd2* transcripts in striatal sections. To characterize the *Oprm1* mRNA distribution in the NAc and DS, we performed triple *in situ* hybridization of *Oprm1*, *Drd1* and *Drd2* in slides of wild-type animals (n=3 mice, 1 section/animal, bilateral evaluation). **(A)** Example of *Oprm1-Drd1* (left) and *Oprm1-Drd2* (right) co-localization, with magnification of double positive cells (insets). **(B, C)** RNAscope analysis **(C)** of NAc (left) and DS (right) selected areas **(B)** reveals that MOR positive neurons are mainly *Drd1* positive, and co-localization with *Drd2* mRNA is also found. Finally, some *Oprm1* transcripts are found in double-labelled *Drd1/Drd2* cells. Very few neurons are expressing *Oprm1* without *Drd1* or *Drd2* transcripts (5.15%±0.39 and 4.70%±0.42 in the NAc and DS respectively). Data are represented as mean + SEM.

Supplemental Figure S2. (A) Whole-brain functional connectivity in live mice using resting-state functional MRI. High resolution spatial independent component analysis followed by partial correlation in time domain and graph theory identifies functional connectivity (FC) hubs displaying above-mean normalized connectivity strength and diversity, which differ across genotypes. This analysis reveals effects of the MOR deletion beyond the VTA-striatum circuit, with however limited alterations at cortical levels. **(B, C, D)** Seed-based directional information flow analysis. **(B)** Location of 6 selected seeds (in yellow) used for C-GC analysis and corresponding slices. **(C)** Matrices show mean C-GC for the 6 seeds in both directions. Horizontal and vertical seeds represent source and destination of information flow, respectively for the lower triangle C-GC and vice-versa for the upper triangle C-GC. Total number of subjects identified by permutation test is shown for each seed-pair. The directional information between DS and VTA target seeds is highlighted within a red square. **(D)** Scheme summarizing dominant (black and orange arrows) or bi-directionality (grey arrows) in Ctl and Dlx-MOR mice for the 6 seed regions, including those forming reward circuits (orange arrows). Hb, habenula; DS, dorsal striatum; NAc, nucleus accumbens; VTA, Ventral tegmental area; PAG, periaqueductal gray; PFC, prefrontal cortex.

Supplemental Figure S3. Naloxone-precipitated withdrawal is unchanged in morphine-dependent Dlx-MOR mice. Individual signs of withdrawal. For the global score and protocol details, see Figure 3D. Data are represented as mean + SEM. Star, significant treatment effect; one star, $p<0.05$; two stars, $p<0.01$; three stars, $p<0.001$.

Supplemental Figure S4. Dopaminergic transmission is unchanged in Dlx-MOR mice. **(A)** Quantitative RT-PCR analysis of *Drd1* and *Drd2* transcripts shows intact expression of DA receptor genes in NAc (left) and DS (right) of Dlx-MOR mice. Transcript levels in mutants are expressed relative to Ctl (dotted line, n=3 to 4), represented as mean + SEM. **(B)** Amphetamine (5 mg/kg, ip) significantly increases locomotor activity (2-h session) in Ctl and Dlx-MOR mice with no significant difference between genotypes (n=6 to 13). Data are represented as mean + SEM. **(C)** Microdialysis shows that cocaine (10 mg/kg at 120 min, 20 mg/kg at 200 min) dose-dependently increases extracellular DA levels above baseline in the NAc of Dlx-MOR and Ctl mice with no genotype effect (n=10 to 14, recording during 380 min). Data are represented as mean + SEM. Sal, saline; Coc, cocaine; #, significant difference with other amphetamine doses; three symbols, $p<0.001$.

Supplemental Figure S5. Implantation sites for microdialysis probes shown in Figure 4B. NAc DA levels were measured in the pre- and post-heroin treatment. The scheme shows probe placement, which was verified by histology for each animal.

Charbogne BPS-D-16-01220R1

In this issue statement

Here we used a conditional gene knockout strategy in mice, to examine whether mu opioid receptors (MORs) expressed in GABAergic forebrain neurons contribute to major biological effects of opiates, and also challenge the VTA-centered canonical disinhibition model of opiate reward. Our data show that: (i) striatal MORs are not necessary for opiate reward, concordant with the two-neuron VTA model, (ii) striatal MORs play a key, yet unreported role in motivated behaviors for both drug and natural rewards and (iii) Dlx-MOR mice represent the first genetic model allowing dissociation of opiate liking and wanting. The study reveals that MORs exert multiple functions throughout brain circuits of reward and motivation.